DEPARTMENT OF ECONOMICS
AND BUSINESS ECONOMICS
AARHUS UNIVERSITY

CREATES
Center for Research in Econometric Analysis of Time Series

The New Keynesian Model and Bond Yields

Martin M. Andreasen

CREATES Research Paper 2021-01

Department of Economics and Business Economics
Aarhus University
Fuglesangs Allé 4
DK-8210 Aarhus V
Denmark

Email: oekonomi@au.dk
Tel: +45 9352 1936

The New Keynesian Model and Bond Yields*

Martin M. Andreasen†

January 7, 2021

Abstract

This paper presents a New Keynesian model to capture the linkages between macro fundamentals and the nominal yield curve. The model explains bond yields with a low level of news in expected inflation and plausible term premia. This implies that the slope of the yield curve predicts future bond returns, and that risk-adjusted historical bond returns satisfy the expectations hypothesis. A key implication of the model is that U.S. bond yields are consistent with demand shocks that are three times less inflationary than implied by a standard log-linearized New Keynesian model estimated without bond yields.

Keywords: Inflation variance ratios, Robust structural estimation, Term premia, The expectations hypothesis, Unspanned macro variation.

JEL: E44, G12.

---

*I thank Kasper Jørgensen, Anders Bredahl Kock, Dennis Kristensen, Giovanni Pellegrino, Morten Ravn, and Daniel Wilhelm for useful comments and discussions. I also appriciate comments from participants at the Cemmap seminar at University College London. I finally acknowledge funding from the Independent Research Fund Denmark, project number 7024-00020B.

†Aarhus University, CREATES, and the Danish Finance Institute. Fuglesangs Allé 4, 8210 Aarhus V, Denmark, email: mandreasen@econ.au.dk, telephone +45 87165982.

1 Introduction

The New Keynesian model is one of the most prominent models in macroeconomics to understand the dynamics of economic activity, inflation, and the monetary policy rate. The model also has implications for prices on financial assets, although these prices often are ignored. The market for nominal government bonds is of particular interest, because bond yields contain information about expected future policy rates and term premia, where the latter is determined by consumption and inflation risk. But, it is well-known that the model struggles to explain bond yields, because its term premia are too low and too stable. This is obviously a concern, because prices are the key device that ensure equilibrium in the model, as emphasized by Cochrane (2007).

Much work has therefore been devoted to improving the New Keynesian model along this dimension. Important contributions are Rudebusch and Swanson (2012) and Kung (2015), which show that stationary productivity shocks and endogenous growth, respectively, allow a New Keynesian model with recursive preferences to generate plausible term premia without distorting macro fundamentals. These extensions imply that news about expected inflation is a key driver of bond yields. However, Duffee (2018) shows that this implication is not consistent with U.S. data, and his finding therefore challenges the current specification of bond yields and inflation in the New Keynesian model.

This paper modifies the New Keynesian model to explain macro fundamentals *and* bond yields with a low level of news in expected inflation. The proposed model is also able to generate realistic term premia that have the same level and variability as in reduced-form dynamic term structure models (DTSMs). In addition, the model satisfies the two requirements in Dai and Singleton (2002) for a correct specification of term premia, which serve as useful diagnostic tests given that term premia are unobserved. The first requirement is that the difference between long- and short-term bond yields (i.e. the yield spread) predicts future bond returns as in Campbell and Shiller (1991). This property of bond yields is evaluated on a long simulated sample and is therefore an unconditional test of term premia. The second requirement is that historical bond returns satisfy the expectations

hypothesis when these returns are adjusted using term premia from the proposed model. This second requirement is therefore a conditional test of term premia, in the sense that it requires reliable state and term premia estimates for historical bond yields.

The key features of our model are recursive preferences and disturbances to the household's utility function that capture demand shocks. These shocks are widely used in macroeconomics, but also in finance following Albuquerque et al. (2016). However, our specification of demand shocks is more flexible than seen previously, as we allow their conditional variance to increase with the level of these shocks. This modification has two important effects. First, it makes demand shocks less inflationary, because even a small rise in uncertainty has a negative impact on inflation with recursive preferences. Second, this weak effect on inflation implies a small response in the policy rate through the Taylor-rule, but the rise in uncertainty increases bond risk premia and generates much larger reponses in longer term yields and therefore a steepening of the yield curve. As a result, demand shocks can generate large variation in medium- and long-term bond yields with only small changes in inflation. This reduces the model's reliance on inflation news to explain bond yields, and demand shocks therefore enable the model to generate inflation variance ratios (as introduced in Duffee (2018)) that are consistent with U.S. data. In contrast, when the conditional variance in demand shocks is constant, we find much larger responses in inflation and the policy rate following demand shocks, but also much smaller responses in medium- and long-term yields. As a result, the model then implies counterfactually large inflation variance ratios.

We show that this new uncertainty channel to explain bond yields is consistent with several other properties of bond yields. First, the positive association between term premia and the yield spread following demand shocks is the key feature that makes the model consistent with the two requirements for a correct specification of term premia. In contrast, when the conditional variance in demand shocks are constant, the yield spread falls after a demand shock, and the model is therefore unable to pass the two requirements for term premia. Second, the model-implied conditional volatilities in bond yields remain consistent with U.S. data. In particular, the model generates plausible Sharpe ratios and implies that the conditional volatility of the ten-year yield predicts annual excess bond returns as seen in the data. The conditional volatilities for U.S. bond yields are

here measured by the EGARCH(1,1) model of Nielson (1991) applied to the change in yields. Third, the nonlinear structure of our model generates a lot of variation in key macro variables that is not explained in linear regressions of these macro variables on bond yields. That is, the model endogenously produces unspanned variation in macro variables as observed in U.S. data, and it therefore avoids the critique of macro-finance term structure models raised in Joslin et al. (2014). Taking the analysis beyond bond yields, we finally show that the yield spread and the price-dividend ratio predict excess returns in equities, as documented by Fama and French (1989). As with bond returns, demand shocks with a time-varying conditional variance are essential to explain these predictability results. Here, and throughout we restrict relative risk aversion to ten, meaning that we do not rely on extreme levels of risk aversion to explain asset prices from macro fundamentals.

By linking financial markets to the macro economy we obtain new insights for both finance and macroeconomics. From a finance perspective, the key insight is that demand shocks are essential for understanding term premia. That is, the asset pricing performance of the New Keynesian model may be improved substantially by including demand shocks along with the supply shocks highlighted in Rudebusch and Swanson (2012) and Kung (2015). From a macroeconomic perspective, the main insight is that the bond market is consistent with demand shocks that are three times less inflationary than implied by a standard log-linearized New Keynesian model estimated without bond yields.

The remainder of this paper is organized as follows. Section 2 presents the New Keynesian model, while our estimation approach is described in Section 3. The main empirical results are provided in Section 4 and robustness is studied in Section 5. Additional model implications are discussed in Section 6 and Section 7 concludes.

2 A New Keynesian Model

2.1 The Households

We consider an infinitely lived representative household with recursive preferences as in Epstein and Zin (1989) and Weil (1990). Using the formulation

in Rudebusch and Swanson (2012), the value function V_t is given by

$$V_t = u_t + \beta \left(\mathbb{E}_t[V_{t+1}^{1-\alpha}] \right)^{1/(1-\alpha)} \tag{1}$$

when the utility function $u_t > 0$ for all t.[1] Here, $\beta \in (0,1)$ is the subjective discount factor and $\mathbb{E}_t[\cdot]$ denotes the conditional expectation in period t. The main purpose of $\alpha \in \mathbb{R} \setminus \{1\}$ is to endow the household with preferences for when uncertainty is resolved, unless $\alpha = 0$ and (1) reduces to expected utility. It follows from Kreps and Porteus (1978) that (1) implies preferences for early (late) resolution of uncertainty if $\alpha > 0$ ($\alpha < 0$) for $u_t > 0$, whereas the opposite sign restrictions apply when $u_t < 0$. Andreasen and Jørgensen (2020) further argue that the size of this timing attitude is proportional to α, meaning that numerically larger values of α generate stronger preferences for early (late) resolution of uncertainty.

The utility function $u_t \equiv u(c_t, l_t)$ is assumed to depend on the number of consumption units c_t bought in the goods market and the provided labor supply l_t to firms. Following Andreasen and Jørgensen (2020), we also include a constant u_0 in the utility function to account for utility from goods and services that are not acquired in the goods market. This could be utility from government spending or utility from goods produced and consumed within the household. As shown in Andreasen and Jørgensen (2020), the reason for introducing u_0 is to separately control the level of the utility function to disentangle the timing attitude α from relative risk aversion (RRA), which otherwise are tightly linked in the standard formulation of recursive preferences.[2] Using a power specification to quantify the utility from market consumption c_t and similarly for leisure $1 - l_t$, we let

$$u(c_t, l_t) = d_t \left[\frac{1}{1-\chi} (c_t - b c_{t-1})^{1-\chi} + z_t^{1-\chi} n_t \varphi_0 \frac{(1-l_t)^{1-\frac{1}{\varphi}}}{1-\frac{1}{\varphi}} + u_0 z_t^{1-\chi} \right]. \tag{2}$$

The parameter $b \geq 0$ accommodates external consumption habits, which are included to capture autocorrelation in consumption growth. The variable d_t introduces shocks to the utility function to temporally increase or decrease the utility from a given level of c_t and l_t, implying that d_t operates as a demand shock.[3] The variable n_t is also exogenous and temporally

[1] When $u_t < 0$, $V_t = u_t - \beta \mathbb{E}_t[(-V_{t+1})^{1-\alpha}]^{\frac{1}{1-\alpha}}$ as in Rudebusch and Swanson (2012).

[2] The Online Appendix shows that our results are robust to restricting $u_0 = 0$ as in the standard implementation of recursive preferences, provided we allow for high RRA.

[3] In the endowment models of Albuquerque et al. (2016) and Gomez-Cram and Yaron

shifts the household's incentive between c_t and l_t, meaning that n_t may be interpreted as a labor supply shock. Market consumption grows with the rate of the productivity level z_t, and it is therefore necessary to scale the utility from leisure and nonmarket consumption by $z_t^{1-\chi}$ to ensure that these terms do not diminish relative to $\frac{1}{1-\chi}\left(c_t - bc_{t-1}\right)^{1-\chi}$ along the balanced growth path. This scaling is discussed and motivated further in Rudebusch and Swanson (2012) and Andreasen and Jørgensen (2020).

The parameter $\chi > 0$ and the degree of habit formation b determine the steady state intertemporal elasticity of substitution (IES) as $\left(1 - b\mu_{z,ss}^{-1}\right)/\chi$, which measures the percentage change in market consumption growth for a one percent change in the real interest rate when ignoring uncertainty. The endogenous labor supply gives the household an additional margin to absorb shocks and this modifies existing expressions for RRA. Using the results in Swanson (2018), it follows that RRA in the steady state is

$$\begin{aligned}\text{RRA} \;=\; & \frac{\chi}{\left(1 - \frac{b}{\mu_{z,ss}}\right) + \chi\varphi\frac{\tilde{w}_{ss}(1-l_{ss})}{\tilde{c}_{ss}}} \\ & + \frac{\alpha\left(1-\chi\right)}{\left(1-\chi\right)u_0\tilde{c}_{ss}^{\chi-1}\left(1 - \frac{b}{\mu_{z,ss}}\right)^{\chi} + \left(1 - \frac{b}{\mu_{z,ss}}\right) + \frac{1-\chi}{1-\frac{1}{\varphi}}\frac{\tilde{w}_{ss}(1-l_{ss})}{\tilde{c}_{ss}}}\end{aligned}$$

where $\tilde{c}_{ss} = c_t/z_t\big|_{ss}$ and $\tilde{w}_{ss} = w_t/z_t\big|_{ss}$ refer to the steady state (ss) of market consumption and the real wage relative to the productivity level. Given that the IES is determined by χ, and α controls the strength of the timing attitude, the level of the utility function u_0 is the key parameter for determining RRA.

The real budget constraint is $c_t + \mathbb{E}_t\left[M_{t,t+1}x_{t+1}^{real}\right] = x_t^{real}/\pi_t + w_t l_t + D_t$. That is, resources are spent on market consumption goods c_t and nominal state-contingent claims X_{t+1}, where $x_{t+1}^{real} \equiv X_{t+1}/P_t$ denotes the real value of these claims that are priced using the nominal stochastic discount factor $M_{t,t+1}$. The household's income is given by the real value of state-contingent claims bought in the previous period x_t^{real}/π_t, the real wage income $w_t l_t$, and real dividend payments from firms D_t. Here, π_t denotes the gross inflation rate.

(forthcoming), shocks to the utility function affect only asset prices and are therefore referred to as capturing valuation risk. In production-based equilibrium models, shocks to d_t generate also endogenous variation in consumption, inflation, etc., and this explains why these shocks are referred to as demand shocks within these models.

2.2 The Firms

Output y_t is produced by a competitive representative firm, which combines differentiated intermediate goods $y_t(i)$ using $y_t = \left(\int_0^1 y_t(i)^{\frac{\eta-1}{\eta}} di\right)^{\frac{\eta}{\eta-1}}$ with $\eta > 1$. The demand for the ith good is given by $y_t(i) = \left(\frac{P_t(i)}{P_t}\right)^{-\eta} y_t$, where $P_t \equiv \left(\int_0^1 P_t(i)^{1-\eta} di\right)^{\frac{1}{1-\eta}}$ denotes the aggregate price level and $P_t(i)$ is the price of the ith good.

Intermediate firms produce slightly differentiated goods using the production function $y_t(i) = z_t a_t k_{ss}^{\theta^f} l_t(i)^{1-\theta^f}$, where k_{ss} and $l_t(i)$ denote capital and labor services at the ith firm, respectively. The variables a_t and z_t capture transitory and permanent productivity shocks. Each intermediate firm can freely adjust its labor demand at the given market wage w_t. Price stickiness is introduced as in Rotemberg (1982), where $\xi \geq 0$ controls the size of firms' real cost $\frac{\xi}{2}\left(P_t(i) / \left(P_{t-1}(i)\pi_{ss}\right) - 1\right)^2 y_t$ when changing $P_t(i)$. As in Rudebusch and Swanson (2012), each firm uses $\delta k_{ss} z_t$ units of output for investment to maintain a constant capital stock along the balanced growth path.

2.3 The Central Bank

The central bank sets r_t according to

$$r_t = r_{ss} + \phi_\pi \log\left(\frac{\pi_t}{\pi_{ss}\pi_t^*}\right) + \phi_c\left(\Delta c_t - \Delta c_{ss}\right), \tag{3}$$

based on a desire to stabilize inflation and economic activity as measured by consumption growth Δc_t. To accommodate deviations in monetary policy from a simple Taylor-rule, we follow the existing literature and introduce an exogenous inflation target π_t^* around the steady state inflation rate π_{ss}.[4]

2.4 Bond Pricing

The price in period t of a default-free zero-coupon bond $B_t^{(k)}$ maturing in k periods with a face value of one dollar is $B_t^{(k)} = \mathbb{E}_t\left[M_{t,t+1} B_{t+1}^{(k-1)}\right]$ for $k = 1, ..., N$ with $B_t^{(0)} = 1$. With continuos compounding, the yield to

[4]Unreported results show no evidence of interest rate smoothing in (3) when the model is estimated using bond yields. This finding is consistent with the results in Rudebusch (2002).

maturity is $r_t^{(k)} = -\frac{1}{k}\log B_t^{(k)}$, where $r_t^{(1)} \equiv r_t$. Bond prices are therefore determined by the nominal stochastic discount factor, which reads

$$M_{t,t+1} = \beta \frac{d_{t+1}}{d_t}\left(\frac{c_{t+1} - bc_t}{c_t - bc_{t-1}}\right)^{-\chi}\left(\frac{\left(\mathbb{E}_t\left[V_{t+1}^{1-\alpha}\right]\right)^{\frac{1}{1-\alpha}}}{V_{t+1}}\right)^{\alpha}\frac{1}{\pi_{t+1}} \tag{4}$$

when $u_t > 0$ for all t. As in Rudebusch and Swanson (2012), the term premium $TP_t^{(k)}$ is defined as the difference between $r_t^{(k)}$ and the corresponding yield under risk-neutral evaluation $\widetilde{r}_t^{(k)}$. That is, $TP_t^{(k)} = r_t^{(k)} - \widetilde{r}_t^{(k)}$ where $\widetilde{r}_t^{(k)} = -\frac{1}{k}\log \widetilde{B}_t^{(k)}$ and $\widetilde{B}_t^{(k)} = e^{-r_t}\mathbb{E}_t\left[\widetilde{B}_{t+1}^{(k-1)}\right]$ with $\widetilde{B}_t^{(0)} = 1$.

2.5 The Structural Shocks

We use standard specifications for four of the five shocks in the model, i.e.

$$\begin{aligned}
\log\left(\mu_{z,t+1}/\mu_{z,ss}\right) &= \rho_{\mu_z}\log\left(\mu_{z,t}/\mu_{z,ss}\right) + \sigma_{\mu_z}\epsilon_{\mu_z,t+1} \\
\log n_{t+1} &= \rho_n \log n_t + \sigma_n \epsilon_{n,t+1} \\
\log \pi^*_{t+1} &= \rho_{\pi^*}\log \pi^*_t + \sigma_{\pi^*}\epsilon_{\pi^*,t+1} \\
\log a_{t+1} &= \rho_a \log a_t + \sigma_a \epsilon_{a,t+1}
\end{aligned} \tag{5}$$

with $\mu_{z,t} \equiv z_t/z_{t-1}$, where $\epsilon_{\mu_z,t+1}$, $\epsilon_{n,t+1}$, $\epsilon_{\pi^*,t+1}$, and $\epsilon_{a,t+1}$ are standard normally distributed and mutually independent across time, denoted $\mathcal{NID}(0,1)$. For demand shocks, the standard assumption of constant conditional variance has a strong impact in the model when households have recursive preferences. This is because these shocks directly affect the amount of uncertainty in the stochastic discount factor, which is a key component for determining term premia. This motivates our slightly more general specification for demand shocks with conditional heteroskedasticity

$$\log d_{t+1} = \rho_d \log d_t + (1 + \omega_d \log d_t)\,\sigma_d \epsilon_{d,t+1}, \tag{6}$$

where $\omega_d \geq 0$ and $\epsilon_{d,t+1} \sim \mathcal{NID}(0,1)$. Thus, the new parameter that we introduce is ω_d, which controls the time-variation in the conditional variance $\mathbb{V}_t\left[\log d_{t+1}\right] = (1 + \omega_d \log d_t)^2\,\sigma_d^2$ of this shock.[5]

[5]Note that the conditional distribution of $\log d_{t+1}$ is Gaussian, and that the conditional variance in (6) is defined in terms of $\log d_t$ and *not* d_t, which ensures that the standard stability condition $|\rho_d| < 1$ applies. Heteroskedasticity plays a much smaller role for the other shocks, and this explains why we use the standard specification in (5).

3 Estimation Methodology

3.1 Data and Model Solution

The model is estimated using quarterly U.S. data from 1961 Q2 to 2007 Q4, where we focus on the period before 2008 to avoid issues related to the zero lower bound for the monetary policy rate. The dynamics of the macro economy is represented by i) labor supply $\log l_t$, ii) consumption growth Δc_t, and iii) inflation.[6] The ten-year nominal yield curve is represented by the three-month, one-year, three-year, five-year, seven-year, and ten-year bond yields. These yields are taken from Gürkaynak et al. (2007), except at the three-month maturity where we use the implied rate on a three-month Treasury Bill. These nine time series are placed in the vector $\mathbf{y}_t^{obs}$ and are expressed in annualized terms except for $\log l_t$.

The state vector for the model is $\mathbf{x}_t = [\ \log d_{t-1} \quad \log c_{t-1} \quad \log \mu_{z,t} \quad \epsilon_{d,t} \quad \log n_t \quad \log \pi_t^* \quad \log a_t\ ]'$. All the remaining variables appear in the vector $\mathbf{y}_t$, including the labor supply, consumption, inflation, and all bond prices. The exact model solution is

$$\begin{aligned} \mathbf{y}_t &= \mathbf{g}(\mathbf{x}_t; \boldsymbol{\theta}) \\ \mathbf{x}_{t+1} &= \mathbf{h}(\mathbf{x}_t; \boldsymbol{\theta}) + \boldsymbol{\eta}\epsilon_{t+1} \end{aligned} \tag{7}$$

with $\epsilon_t = \left[\ \epsilon_{\mu_z,t} \quad \epsilon_{d,t} \quad \epsilon_{n,t} \quad \epsilon_{\pi^*,t} \quad \epsilon_{a,t}\ \right]'$, which we solve by a third-order perturbation approximation around the steady state.[7]

3.2 Robustified Inference with Nonlinear Filtering

The approximated state space representation of the model includes nonlinear terms with the unobserved states $\mathbf{x}_t$, implying that the Kalman filter cannot be used to estimate the model. Instead, we rely on the central difference Kalman filter (CDKF) developed by Norgaard et al. (2000), which is a nonlinear extension of the Kalman filter. The CDKF accommodates measurement errors in $\mathbf{y}_t^{obs}$, and we specify these errors $\mathbf{v}_t$ to be uncorrelated Gaussian white noise, as typically assumed when estimating struc-

[6] The labor supply is measured by the total number of employees for total nonfarm payrolls, which is detrended using the procedure in Hamilton (2018). The consumption growth rate is calculated from real per capita nondurables and service expenditures. Inflation is measured by the year-on-year growth rate in the consumer price index (CPI) excluding food and energy prices for all urban consumers.

[7] All equilibrium conditions in the model are derived in the Online Appendix.

tural macro models and reduced-form DTSMs. That is, $\mathbf{v}_t \sim \mathcal{NID}(\mathbf{0}, \mathbf{R}_\mathbf{v})$ where $\mathbf{R}_\mathbf{v}$ is a diagonal covariance matrix, implying that $\mathbf{y}_t^{obs} = \mathbf{S}\mathbf{y}_t + \mathbf{v}_t$ for an appropriate selection matrix $\mathbf{S}$.[8]

A likelihood function can be derived from the CDKF under the assumption that the prediction errors for $\mathbf{y}_t^{obs}$ are Gaussian. However, this distributional specification does not hold exactly due to the nonlinear terms in the model solution. The CDKF therefore only provides a quasi log-likelihood function $\frac{1}{T}\sum_{t=1}^{T}\mathcal{L}_t(\boldsymbol{\theta})$, which can be used for a quasi maximum likelihood (QML) estimation, as suggested in Andreasen (2013).

A possible limitation of any QML approach (as with standard maximum likelihood) is its lack of robustness to model misspecifications other than the distributional assumption of the prediction errors for $\mathbf{y}_t^{obs}$. An obvious possible source of misspecification in the New Keynesian model is that the same structural parameter $\boldsymbol{\theta}$ determines the **g**- and the **h**-function. In contrast, the widely used reduced-form Gaussian DTSM basically allows these two functions to be determined by separate parameters, which in these models is essential to generate term premia dynamics that are not rejected by historical data (see Dai and Singleton (2002)).[9] In the context of the New Keynesian model, the **g**-function is likely to prefer large and persistent shocks, because this helps the model generate variation in term premia and hence fit medium- and long-term bond yields. On the other hand, small and less persistent shocks are typically needed in the **h**-function to fit the state dynamics and ensure sensible unconditional properties of $\mathbf{y}_t^{obs}$. Given the inclusion of several bond yields with relatively small measurement errors in the estimation, our experience is that the **g**-function dominates the QML estimates of the New Keynesian model. This typically implies a close in-sample fit to $\mathbf{y}_t^{obs}$, but it comes at the expense of unconditional variances for $\mathbf{y}_t^{obs}$ that are too large compared to U.S. data.

Thus, a robustified version of the standard QML estimator is required to obtain reliable estimates of our New Keynesian model. The solution

[8] Unlike the more accurate particle filter proposed in Fernández-Villaverde and Rubio-Ramírez (2007), the updating rule for the states in the CDKF is linear, implying that the recursive filtering equations only depend on first and second moments. The CDKF approximates these moments by a deterministic sampling procedure, and this makes the CDKF computationally much faster than any particle filter and generally also more accurate than the well-known extended Kalman filter.

[9] The only link between the **g**- and **h**-functions in the reduced-form Gaussian DTSM is the conditional covariance matrix of the states, but the effect of this covariance matrix on the **g**-function is typically very small.

we propose is to shrink the QML estimator to the unconditional first and second moments of $\mathbf{y}_t^{obs}$, because this is a simple and transparent way to increase the weight assigned to the $\mathbf{h}$-function in the estimation. We denote the shrinkage moments by $\frac{1}{T}\sum_{t=1}^{T}\mathbf{m}_t$ in the sample and by $\mathbb{E}\left[\mathbf{m}\left(\boldsymbol{\theta}\right)\right]$ in the model. The applied estimator is given by

$$\hat{\boldsymbol{\theta}} = \underset{\boldsymbol{\theta}\in\boldsymbol{\Theta}}{\arg\max}\ \frac{1}{T}\sum_{t=1}^{T}\mathcal{L}_t\left(\boldsymbol{\theta}\right) - \lambda\mathbf{f}_{1:T}\left(\boldsymbol{\theta}\right)'\mathbf{W}\mathbf{f}_{1:T}\left(\boldsymbol{\theta}\right), \tag{8}$$

where $\boldsymbol{\Theta}$ is the feasible domain of $\boldsymbol{\theta}$, $\mathbf{f}_{1:T}\left(\boldsymbol{\theta}\right) \equiv \frac{1}{T}\sum_{t=1}^{T}\mathbf{f}_t\left(\boldsymbol{\theta}\right)$ with $\mathbf{f}_t\left(\boldsymbol{\theta}\right) \equiv \mathbf{m}_t - \mathbb{E}\left[\mathbf{m}\left(\boldsymbol{\theta}\right)\right]$, and $\mathbf{W}$ is a diagonal weighting matrix containing the inverse of the standard errors for the shrinkage moments.[10]

The nature of the estimator in (8) is determined by $\lambda \geq 0$, which controls the weight assigned to the shrinkage moments relative to the sample average of $\mathcal{L}_t\left(\boldsymbol{\theta}\right)$. We obviously recover the standard QML estimator when $\lambda = 0$, while $\hat{\boldsymbol{\theta}}$ converges to the generalized methods of moments (GMM) estimator in Hansen (1982) when λ becomes sufficiently large. We consider a small amount of shrinkage by letting $\lambda = T$, which in our setting implies that shrinkage constitutes a fairly small part of the objective function, typically about 5% to 10%. Our results are not particularly sensitive to increasing the degree of shrinkage further, although we do find notable effects of shrinkage when compared to the standard QML estimator.[11]

To obtain closed-form expressions for the model-implied shrinkage moments, we apply the pruning scheme of Andreasen et al. (2018) when setting up the state space system for the approximated version of the model.[12] This implies that the estimator in (8) can be implemented without resorting to simulation and belongs to the general class of extremum estimators. Its asymptotic properties are therefore easily derived in the Online Appendix.

We use two classes of shrinkage moments. The first class contains first and second unconditional moments of $\mathbf{y}_t^{obs}$, except for the mean of de-

[10] Another possibility is to use the optimal weigthing matrix, but this version of (8) is not considered to avoid well-known small-sample distortions from estimating large covariance matrices in moment-based estimators.

[11] Note also that (8) belongs to the class of Laplace type or quasi-Bayesian estimators of Chernozhukov and Hong (2003), where a potentially misspecified log-likelihood function (as considered in our case) may be used within a Bayesian setting. When this estimator is combined with the endogenours prior specification in Christiano et al. (2011) using a pre-sample of length T^*, we obtain the objective function in (8) with $\lambda = T^*/2$.

[12] The pruning scheme is not essential in our case, because the proposed model has only one endogenous state (i.e. $\log c_{t-1}$), and partly for this reason appears to be fairly stable when simulated without pruning.

trended labor supply that is approximately zero. These moments help to robustify the QML estimates, which is illustrated in a Monte Carlo study in the Online Appendix. Here we show that shrinkage towards these moments give smaller parameter biases and more reliable inference than standard QML when the model is misspecified with the **g**- and **h**-functions determined by different structural parameters. On the other hand, without any model misspecification, we unexpectedly find no benefit of shrinkage, which mainly reduces the efficiency of the standard QML estimator that is nearly unbiased and provides reliable inference in this case. We benchmark these results to using an extreme degree of shrinkage with $\lambda = 10^6$, which corresponds to estimating the structural parameters by GMM and obtaining the states afterwards by the CDKF. The Monte Carlo study shows that these GMM estimates display notable biases in finite samples and are clearly less efficient compared to the standard QML estimator ($\lambda = 0$) and the proposed estimator (with $\lambda = T$), both with and without model misspecification. These imprecise GMM estimates of the structural parameters also imply less accurate state estimates when compared to the proposed estimator with $\lambda = T$.

The second class of moments we include contain information about term premia as captured by the regression of Campbell and Shiller (1991). That is,

$$r_{t+m}^{(k-m)} - r_t^{(k)} = \alpha_k + \beta_k \frac{m}{k-m}\left(r_t^{(k)} - r_t^{(m)}\right) + u_{t+m,k}, \tag{9}$$

where $u_{t+m,k}$ is an error term and $m = 4$ to obtain yearly changes in bond yields. The expectations hypothesis implies $\beta_k = 1$, but empirical estimates of the regression loadings β_k are negative and decreasing with maturity, which is evidence of time-varying term premia. This implies that bond returns are predictable, because (9) is equivalent to the predictability regression $rx_{t+m}^{(k)} = \tilde{\alpha}_k + \tilde{\beta}_k\left(r_t^{(k)} - r_t^{(m)}\right) + \varepsilon_{t+m,k}$, where $rx_{t+m}^{(k)}$ is excess returns and $\tilde{\beta}_k \equiv \frac{m}{4}(1-\beta_k)$. We consider β_k at the three-, five-, seven-, and ten-year maturity to assign more weight to the evidence against the expectations hypothesis than implied by the considered panel of bond yields used to compute the quasi log-likelihood function. These loadings are represented in the shrinkage moments by including $Cov(r_{t+m}^{(k-m)} - r_t^{(k)}, r_t^{(k)} - r_t^{(m)})$ and $Var(r_t^{(k)} - r_t^{(m)})$ related to β_k at the four considered maturities.

3.3 Calibrated Parameters

Not all parameters in the New Keynesian model are well-identified from $\mathbf{y}_t^{obs}$, and they are therefore determined by standard calibration arguments. Hence, we let $\delta = 0.025$, $l_{ss} = 0.33$, and $\theta^f = 0.4$ as typically assumed for the U.S. economy. We also consider an average price markup of 20% with $\eta = 6$, and we set the ratio of capital to output in the steady state to 2.5 as in Rudebusch and Swanson (2012). The value of $\mu_{z,ss}$ is set to match the mean of consumption growth, implying that $\mu_{z,ss} = 1.0055$. Most micro estimates of the Frisch labor supply elasticity for males are in the range from 0.10 to 0.40 according to Keane (2011). To help the New Keynesian model generate low variability in the labor supply, we consider a Frisch elasticity in the lower part of this interval by letting $\varphi = 0.075$, which implies a Frisch elasticity of $\varphi\left(1/l_{ss} - 1\right) = 0.15$ in the steady state.

Given this calibration of φ and our finding below that χ is larger than one, the utility function in (2) is negative. Hence, the parameter α characterizing the recursive preferences in (1) must be negative to generate preferences for early resolution of uncertainty. The model's goodness of fit generally improves the more negative α gets, but the performance gain trails off when α gets below -40 in our case.[13] We therefore simply let $\alpha = -40$, which also ensures a low and plausible level of the timing premium as introduced in Epstein et al. (2014). We finally set the constant u_0 to get a steady state RRA of ten as in Bansal and Yaron (2004).

The size of the measurement errors in $\mathbf{y}_t^{obs}$ have a relatively small effect on the estimates, and we therefore simply assume that 10% of the variation in the three macro variables is due to measurement errors. This implies measurement errors with standard deviations of i) 27 basis points for the labor supply, ii) 17 basis points for consumption growth, and iii) 27 basis points for inflation. The standard deviation for the measurement errors in all bond yields is set to 5% of the average standard deviations in the six considered yields, which corresponds to 13 basis points.

4 Estimation Results

This section presents the main results for the proposed model. We proceed by discussing the estimated parameters and the fit in Section 4.1 to Section

[13] Rudebusch and Swanson (2012) report a similar property in their model.

4.3. The following three subsections explore how well the model matches key moments of bond yields that are *not* included in the estimation. The key mechanisms in the model are explained in Section 4.7.

4.1 Estimated Parameters and Model Fit

The first column in Table 1 reports the estimated parameters in our preferred version of the model. This model is denoted $\mathcal{M}^{M,CS}$, where the superscripts indicate that shrinkage is applied based on the considered first and second unconditional moments of $\mathbf{y}_t^{obs}$ (by "M") and the selected Campbell-Shiller moments (by "CS"). The results for the other versions of the model, denoted $\mathcal{M}^{M}$ and $\mathcal{M}$, will be discussed below in Section 5.1. For our preferred model $\mathcal{M}^{M,CS}$, we find a moderate degree of habit formation with $\hat{b} = 0.21$. This generates autocorrelation in consumption growth with $corr\left(\Delta c_t, \Delta c_{t-1}\right) = 0.24$, which is close to the corresponding sample moment of 0.40. For the curvature parameter in the utility function, we find $\hat{\chi} = 4.19$, which together with the estimate of b imply an IES of 0.19. This relatively low IES is consistent with Hall (1988) and Yogo (2004), who estimate the IES to between zero and 0.2. To aid the interpretation of the price adjustment parameter ξ, Table 1 reports the corresponding Calvo parameter $\hat{\xi}_{Calvo}$ that gives the same slope of the aggregate supply relation as $\hat{\xi}$ when linearizing this relation.[14] We find $\hat{\xi}_{Calvo} = 0.75$, which corresponds to an average duration for prices of four quarters. The central bank assigns more weight to stabilizing inflation than economic activity with $\hat{\phi}_{\pi} = 5.85$ and $\hat{\phi}_{\Delta c} = 0.23$. Although this is a common finding, the value of ϕ_{π} is somewhat higher than typically reported in the literature but also estimated very imprecisely in our case, where $\hat{\phi}_{\pi}$ has a standard error of 1.52. Thus, in the Online Appendix we show that the implications from $\mathcal{M}^{M,CS}$ are basically unaffected when reducing ϕ_{π} to three, which is more standard when using a third-order approximation (see, for instance, Andreasen et al. (2018)).

Permanent productivity shocks and the inflation target are found to be highly persistent ($\hat{\rho}_{\mu_z} = 0.965$ and $\hat{\rho}_{\pi^*} = 0.988$) and with small innovations ($\hat{\sigma}_{\mu_z} = 3.3 \times 10^{-4}$ and $\sigma_{\pi^*} = 7.8 \times 10^{-4}$), meaning that $\mu_{z,t}$ and π_t^* capture real and nominal long-run risk as in Bansal and Yaron (2004) and

[14] The mapping between ξ and ξ_{Calvo} is $\xi = \frac{(1-\theta+\eta\theta)(\eta-1)\xi_{Calvo}}{(1-\xi_{Calvo})(1-\theta)\left(1-\xi_{Calvo}\beta\mu_{z,ss}^{1-\frac{1}{\psi}}\right)}$.

Table 1: The Structural Parameters

This table shows the estimated structural parameters using data from 1961 Q2 to 2007 Q4, with asymptotic standard errors provided in parenthesis. The first four observations are used to initialize the CDKF. When shrinkage is applied in the estimation, as denoted by the superscripts M and CS on the model object $\mathcal{M}$, an equal weighting between moments related to the three macro variables (i.e. $\log l_t$, Δc_t, and π_t) and moments related to the yield curve (i.e. six bond yields and eight moments to capture the four Campbell-Shiller loadings) is targeted by correcting for the number of included moments. Hence, for $\mathcal{M}^{M,CS}$ the weights assigned to each of the macro moments are upscaled by four, whereas they are upscaled by 2.5 for $\mathcal{M}^{M}$. No standard error is provided for β when this parameter is at the upper bound of 0.9995. The timing premium is evaluated at the steady state and computed as in Andreasen and Jørgensen (2020).

	(1) $\mathcal{M}^{M,CS}$	(2) $\mathcal{M}^{M}$	(3) $\mathcal{M}$
β	0.9995	0.9995	0.9992
	–	–	(0.003)
b	0.214	0.220	0.465
	(0.070)	(0.071)	(0.009)
χ	4.193	4.728	6.861
	(0.634)	(0.968)	(0.031)
ξ_{Calvo}	0.747	0.735	0.541
	(0.041)	(0.04)	(0.017)
ϕ_π	5.846	5.566	3.479
	(1.517)	(0.918)	(0.037)
$\phi_{\Delta c}$	0.227	0.273	0.391
	(0.130)	(0.143)	(0.035)
ρ_{μ_z}	0.965	0.947	0.945
	(0.011)	(0.008)	(0.004)
ρ_d	0.954	0.945	0.961
	(0.005)	(0.006)	(0.002)
ρ_n	0.987	0.986	0.996
	(0.009)	(0.008)	(0.002)
ρ_{π^*}	0.988	0.982	0.992
	(0.007)	(0.004)	(0.003)
ρ_a	0.988	0.982	0.985
	(0.037)	(0.013)	(0.002)
π_{ss}	1.015	1.016	1.032
	(0.002)	(0.001)	(0.002)
$\sigma_{\mu_z} \times 100$	0.033	0.042	0.037
	(0.006)	(0.007)	(0.002)
σ_d	0.051	0.054	0.049
	(0.002)	(0.002)	(0.002)
σ_n	0.042	0.046	0.092
	(0.011)	(0.012)	(0.007)
$\sigma_{\pi^*} \times 100$	0.078	0.090	0.124
	(0.024)	(0.017)	(0.029)
σ_a	0.003	0.004	0.015
	(0.001)	(0.001)	(0.001)
ω_d	0.653	0.716	0.367
	(0.152)	(0.265)	(0.064)
Timing Premium	11%	10%	7%
IES	0.19	0.17	0.08
RRA	10	10	10
u_0	-9.8	-11.3	-264.4

Rudebusch and Swanson (2012), respectively. The demand shocks are also fairly persistent with $\hat{\rho}_d = 0.954$, and they display heteroskedasticity with $\hat{\omega}_d = 0.653$, which clearly is significantly different from zero. Thus, the

Table 2: Goodness of Insample Fit

Panel $\mathcal{A}$ shows the full sample estimate of the standard deviations of the measurement errors when reported in annualized basis points. The numbers in parenthesis refer to an alternative estimate of these standard deviations robust to outliers, where observations below the 2.5 and above the 97.5 percentiles are removed. Both standard deviations are computed using the posterior state estimates from the CDKF. Panel $\mathcal{B}$ shows a decomposition of the objective function $\mathcal{L} \equiv \mathcal{L}^{CDKF} + Q^{GMM}$, where $\mathcal{L}^{CDKF} \equiv \frac{1}{T}\sum_{t=1}^{T} \mathcal{L}_t(\boldsymbol{\theta})$ and $Q^{GMM} \equiv -\lambda \mathbf{f}_{1:T}(\boldsymbol{\theta})' \mathbf{W} \mathbf{f}_{1:T}(\boldsymbol{\theta})$.

	(1) $\mathcal{M}^{M,CS}$	(2) $\mathcal{M}^{M}$	(3) $\mathcal{M}$
Panel $\mathcal{A}$: Measurement errors			
$std\left(\hat{l}_t\right)$	30.0 (22.1)	28.0 (20.5)	29.0 (9.9)
$std\left(\Delta c_t\right)$	12.7 (7.4)	11.4 (6.6)	14.4 (4.7)
$std\left(\pi_t\right)$	28.4 (18.7)	23.0 (15.3)	59.0 (25.4)
$std\left(r_t\right)$	30.1 (17.6)	28.8 (15.7)	187.3 (59.6)
$std\left(r_t^{(4)}\right)$	22.8 (16.4)	22.3 (16.1)	49.8 (18.5)
$std\left(r_t^{(12)}\right)$	14.8 (12.5)	13.8 (11.7)	18.5 (7.7)
$std\left(r_t^{(20)}\right)$	8.5 (7.1)	10.2 (8.3)	14.3 (6.4)
$std\left(r_t^{(28)}\right)$	7.3 (5.3)	7.9 (5.2)	10.0 (4.6)
$std\left(r_t^{(40)}\right)$	13.0 (11.4)	15.4 (13.4)	9.7 (8.4)
Panel $\mathcal{B}$: Objective function			
$\mathcal{L}^{CDKF}$	30.7	31.8	36.1
Q^{GMM}	−2.4	−0.8	0
$\mathcal{L}$	28.4	31.0	36.1

proposed extension of demand shocks in (6) is strongly supported by the data. We also find a realistic timing premium of 11%, meaning that the household is willing to give up 11% of total lifetime consumption to have all uncertainty resolved in the following period.

Table 2 reports the standard deviations of the measurement errors $\mathbf{v}_t$ and reveals a close fit to the three macro variables and the six bond yields despite using only five shocks in the model. These standard deviations are between 8 and 30 basis points for bond yields, or when abstracting from outliers between 5 and 18 basis points, as seen from the figures in parenthesis. The bottom panel in Table 2 further shows that the applied shrinkage in $\mathcal{M}^{M,CS}$ has a small effect on the optimal value of the objective function, where the GMM moment conditions due to shrinkage only account for about 8% (i.e. 2.4/28.4) of its value.

4.2 Unconditional Stylized Moments

Table 3 explores the ability of $\mathcal{M}^{M,CS}$ to match the unconditional means and standard deviations in $\mathbf{y}_t^{obs}$ as included when estimating $\mathcal{M}^{M,CS}$. The first column in Table 3 shows U.S. sample moments (and their bootstrapped 95% confidence bands), while the second column shows the corresponding population moments in $\mathcal{M}^{M,CS}$. We first note that $\mathcal{M}^{M,CS}$ reproduces the mean level of inflation and all bond yields. For instance, the level of the three-month yield is 5.68% vs. 5.59% in the data, and the level of the ten-year bond yield is 6.97% vs. 6.99% in the data. This implies that the average yield spread is 129 basis points in $\mathcal{M}^{M,CS}$ compared to 140 basis points in historical data.

The model is also successful in matching the standard deviation of labor supply (3.04% vs. 2.73% in the data), consumption growth (1.88% vs. 1.72% in the data), and inflation (2.66% vs. 2.65% in the data). The standard deviations of bond yields are also well matched, where the model captures the negative association between these standard deviations and maturity. Thus, $\mathcal{M}^{M,CS}$ explains both the level and variability of the data.[15]

4.3 Ordinary Campbell-Shiller Loadings

Next, we explore whether $\mathcal{M}^{M,CS}$ can match the empirical pattern in the ordinary Campbell-Shiller loadings β_k from (9), which we include in the estimation at the three-, five-, seven-, and ten-year maturity. Figure 1 plots these loadings in the sample along with their bootstrapped 95% confidence bands. A very encouraging finding is that $\mathcal{M}^{M,CS}$ generates ordinary Campbell-Shiller loadings that are *negative* and tract the empirical loadings remarkably well inside their 95% confidence bands. This shows that the model satisfies the first requirement for a correct specification of term premia. In contrast, imposing $\omega_d = 0$ in $\mathcal{M}^{M,CS}$ generates *positive* Campbell-Shiller loadings around two.

[15] Following the work of Piazzesi and Schneider (2007), the correlation between π_t and Δc_t has also attrated some attention in the literature. We find $corr(\pi_t, \Delta c_t) = 0.03$ in $\mathcal{M}^{M,CS}$ and $corr(\pi_t, \Delta c_t) = -0.27$ in our sample from 1961 Q2 to 2007 Q4. However, a negative correlation between π_t and Δc_t is not a robust feature of U.S. data as emphasized by Benigno (2007). For instance, extending the sample to 2019 Q3 implies $corr(\pi_t, \Delta c_t) = -0.12$, while $corr(\pi_t, \Delta c_t) = 0.10$ in a sample from 1985 Q1 to 2019 Q3.

Table 3: Unconditional First and Second Moments

The data moments are for the U.S. from 1961 Q2 to 2007 Q4 with 95% confidence bands stated below. These bands are computed using a block bootstrap with 100,000 bootstrap samples using blocks of 60 observations. The model-implied moments are computed in closed form based on Andreasen et al. (2018). All means and standard deviations are stated in annualized percent, except for the standard deviation of $\hat{l}_t$ which is not annualized.

	(1) Data	(2) $\mathcal{M}^{M,CS}$	(3) $\mathcal{M}^{M}$	(4) $\mathcal{M}$
Means				
Δc_t	2.20 [1.90,2.49]	2.20	2.20	2.20
π_t	4.25 [2.30,6.19]	4.35	4.31	6.78
r_t	5.59 [3.72,7.46]	5.68	5.64	7.52
$r_t^{(4)}$	6.11 [4.06,8.15]	5.96	5.90	7.78
$r_t^{(12)}$	6.47 [4.43,8.52]	6.49	6.37	7.51
$r_t^{(20)}$	6.68 [4.66,8.70]	6.78	6.65	7.36
$r_t^{(28)}$	6.83 [4.84,8.82]	6.92	6.82	7.36
$r_t^{(40)}$	6.99 [5.04,8.95]	6.97	6.97	7.51
Stds				
$\hat{l}_t$	2.73 [2.24,3.22]	3.04	3.07	10.45
Δc_t	1.72 [1.44,2.01]	1.88	1.90	3.71
π_t	2.65 [1.45,3.86]	2.66	2.55	6.11
r_t	2.71 [1.72,3.71]	3.03	3.25	9.30
$r_t^{(4)}$	2.82 [1.83,3.80]	3.02	3.18	7.11
$r_t^{(12)}$	2.65 [1.68,3.63]	3.04	3.10	6.48
$r_t^{(20)}$	2.55 [1.58,3.52]	3.02	3.03	6.18
$r_t^{(28)}$	2.48 [1.51,3.45]	2.97	2.91	5.93
$r_t^{(40)}$	2.41 [1.46,3.37]	2.82	2.67	5.60

4.4 Risk-Adjusted Campbell-Shiller Loadings

Next, we study moments that are not included in the estimation of $\mathcal{M}^{M,CS}$. A correct specification of term premia should imply that historical risk-adjusted bond yields satisfy the expectations hypothesis. Dai and Singleton (2002) show that this corresponds to testing whether the loading β_k^{Adj} is

Figure 1: Ordinary Campbell-Shiller Loadings
This figure shows the ordinary Campbell-Shiller regression loadings β_k for $m = 4$. The empirical values are computed using U.S. data from 1961 Q2 to 2007 Q4. The shaded area denotes the 95 percent confidence interval for these estimates, computed using a block bootstrap where the regressand and the regressor in (9) are sampled jointly in blocks of 10 observations in 100,000 bootstrap samples. The model-implied Campbell-Shiller loadings are computed in closed form using the results in Andreasen et al. (2018).

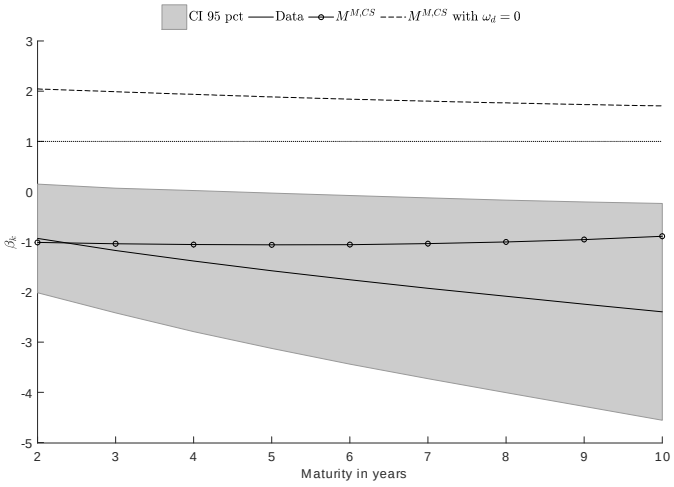

equal to one in the following version of the Campbell-Shiller regression

$$\begin{aligned} & r_{t+m}^{(k-m)} - r_t^{(k)} - \left(\widetilde{TP}_{t+m}^{(k-m)} - \widetilde{TP}_t^{(k-m)}\right) + \frac{m}{k-m} TP_t^{fwd,(k-m)} \quad (10) \\ = \; & \alpha_k^{Adj} + \beta_k^{Adj} \frac{m}{k-m}\left(r_t^{(k)} - r_t^{(m)}\right) + u_{t+m,k}^{Adj}, \end{aligned}$$

where term premia are subtracted from long-term yields. Here, $\widetilde{TP}_t^{(k)} = r_t^{(k)} - \frac{1}{k}\sum_{i=0}^{k-1} \mathbb{E}_t\left[r_{t+i}\right]$ is another commonly used definition of term premium, that only differs from $TP_t^{(k)}$ by including a small convexity term. The variable $TP_t^{fwd,(k)} = f_{t,k} - \mathbb{E}_t\left[r_{t+k}\right]$ is the term premium in the forward rate $f_{t,k} \equiv -\log\left(B_t^{(k+1)}/B_t^{(k)}\right)$ and $u_{t+m,k}^{Adj}$ is an error term.

Figure 2 uses term premia from $\mathcal{M}^{M,CS}$ to compute risk-adjusted Campbell-Shiller loadings β_k^{Adj} and their 95% confidence bands on the historical sample from 1961 Q2 to 2007 Q4. Very encouragingly, we find that all these loadings are close to one, and that the 95% confidence bands for these estimates always contain the desired value of one. This shows that term premia from our model are not rejected by the data, implying that it also passes the second requirement for a correct specification of term premia. On the other hand, imposing $\omega_d = 0$ in $\mathcal{M}^{M,CS}$ implies values of β_k^{Adj} that

Figure 2: Risk-Adjusted Campbell-Shiller Loadings

The figure shows the risk-adjusted Campbell-Shiller regression loadings β_k^{Adj} for $m = 4$ in U.S. data from 1961 Q2 to 2007 Q4 when using the term premium from $\mathcal{M}^{M,CS}$. The shaded area denotes the 95 percent confidence interval for these estimates, computed using a block bootstrap where the regressand and the regressor in (10) are sampled jointly in blocks of 10 observations in 100,000 bootstrap samples.

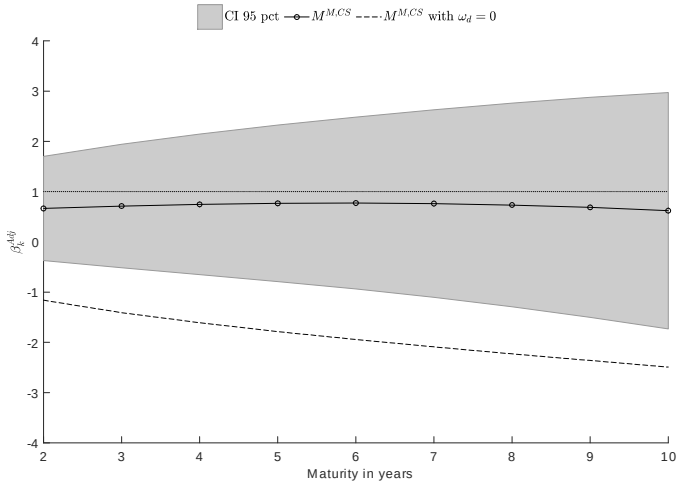

are negative and significantly different from one.

4.5 Inflation News in Bond Yields

Duffee (2018) shows that the quarterly news in bond yields $\tilde{r}_t^{(k)} = r_t^{(k)} - \mathbb{E}_{t-1}\left[r_t^{(k)}\right]$ is much more volatile than the quarterly news in expected inflation $\eta_{\pi,t}^{(k)} = \mathbb{E}_t\left[\frac{1}{k}\sum_{i=1}^{k}\pi_{t+i}\right] - \mathbb{E}_{t-1}\left[\frac{1}{k}\sum_{i=1}^{k}\pi_{t+i}\right]$. The inflation variance ratio $VR_\pi^{(k)} = \mathbb{V}[\eta_{\pi,t}^{(k)}]/\mathbb{V}[\tilde{r}_t^{(k)}]$ is therefore only around 0.15 in the U.S., whereas this ratio often exceeds one in various versions of the New Keynesian model (see Duffee (2018)). However, the time series for $\tilde{r}_t^{(k)}$ and $\eta_{\pi,t}^{(k)}$ in the U.S. display clear evidence of time-varying volatility, and Gomez-Cram and Yaron (forthcoming) therefore refine the estimates in Duffee (2018) by correcting for heteroskedasticity. This increases $VR_\pi^{(k)}$ to 0.23, 0.22, and 0.19 at the one, three, and five year maturity, as shown in Table 4.[16] The proposed model $\mathcal{M}^{M,CS}$ implies that the standard deviation in news to expected inflation is only about 0.3 and hence substantially lower than the standard deviation in news to bond yields of about 0.6. The model therefore implies fairly low inflation variance ratios of 0.32, 0.28, and 0.25

[16] We are grateful to Roberto Gomez-Cram for sharing these data moments.

Table 4: News to Inflation and Bond Yields

This table reports the annualized standard deviation of quarterly news in expected inflation $\eta_{\pi,t}^{(k)} = \mathbb{E}_t\left[\frac{1}{k}\sum_{i=1}^{k}\pi_{t+i}\right] - \mathbb{E}_{t-1}\left[\frac{1}{k}\sum_{i=1}^{k}\pi_{t+i}\right]$ in percent, the annualized standard deviation of quarterly news in bond yields $\tilde{r}_t^{(k)} = r_t^{(k)} - \mathbb{E}_{t-1}\left[r_t^{(k)}\right]$ in percent, and the inflation variance ratio $VR_\pi^{(k)} = \mathbb{V}[\eta_{\pi,t}^{(k)}]/\mathbb{V}[\tilde{r}_t^{(k)}]$. The data moments are from Gomez-Cram and Yaron (forthcoming) (supported material provided by R. Gomez-Cram) with a correction for heteroskedasticity. These estimates are from 1962 Q1 to 2018 Q4, where the standard deviations in bond yields news use martingale forecasts, and the standard deviations in expected inflation news are obtained using the GDP deflator and surveys on current-quarter inflation. Figures in parenthesis denote the 90 percent credibility interval. The corresponding model-implied moments are computed for the indicated versions of the New Keynesian model. News to expected inflation $\eta_{\pi,t}^{(k)}$ and news in bond yields $\tilde{r}_t^{(k)}$ are computed directly by the third-order perturbation approximation, while the unconditional standard deviations of $\eta_{\pi,t}^{(k)}$ and $\tilde{r}_t^{(k)}$ are obtained using the closed form expression provided in Andreasen et al. (2018).

	(1) Data	(2) $\mathcal{M}^{M,CS}$	(3) $\mathcal{M}^{M}$	(4) $\mathcal{M}$
Std of inflation news				
1-year	0.22 [0.19,0.25]	0.36	0.42	0.76
3-year	0.21 [0.18,0.24]	0.34	0.39	0.68
5-year	0.20 [0.18,0.23]	0.33	0.36	0.65
10-year	-	0.29	0.30	0.59
Std of yield news				
1-year	0.46 [0.41,0.51]	0.64	0.86	2.81
3-year	0.44 [0.40,0.50]	0.65	0.83	1.55
5-year	0.46 [0.41,0.51]	0.66	0.81	1.30
10-year	-	0.62	0.71	1.05
Inflation variance ratio				
1-year	0.23 [0.16,0.32]	0.32	0.24	0.07
3-year	0.22 [0.16,0.32]	0.28	0.22	0.20
5-year	0.19 [0.14,0.27]	0.25	0.20	0.25
10-year	-	0.22	0.18	0.31

at the one, three, and five year maturity, respectively, which all are within the reported 90% uncertainty bands for the corresponding data moments in Table 4. This shows that the proposed New Keynesian model is able to address the recent critique of Duffee (2018). As with the risk-adjusted Campbell-Shiller loadings in Section 4.4, we emphasize that the model's ability to explain the inflation variance ratios is an out-of-sample test, in the sense that β_k^{Adj} and $VR_\pi^{(k)}$ are not included in the model estimation.

4.6 Term Premia

The ten-year term premium implied by $\mathcal{M}^{M,CS}$ is shown at the top of Figure 3, where the shaded bars denote NBER recessions. The figure reveals that the model generates the same overall pattern for nominal term premia as found in the flexible five-factor model of Adrian et al. (2013), which is a standard reduced-form Gaussian DTSM without any economic structure imposed on the stochastic discount factor. The correlation between the two measures of term premia is 85%, with the similarities being particularly strong after the mid 1980s.[17] Note also that both measures generally increase during NBER recessions and hence capture the counter-cyclical nature of bond risk premia. The summary statistics for term premia are also very similar across the two models, as the ten-year nominal term premium in $\mathcal{M}^{M,CS}$ has a mean of 172 basis points and a standard deviation of 139 basis points, while the corresponding moments are 180 and 125 basis points, respectively, in the model of Adrian et al. (2013).

The bottom of Figure 3 reports a shock decomposition of the ten-year term premium, exploiting that $TP^{(k)}$ is linear in the states for our approximation. We find that demand shocks explain 65% of the variation of this term premium, while permanent productivity shocks $\mu_{z,t}$ account for 16% of its variation. Shocks to the inflation target also account for 16% and contribute mainly to the elevated level of term premia from the mid 1970s to the mid 1980s.

4.7 Understanding the Key Mechanisms in the Model

At this point, we have shown that the proposed model i) explains historical bond yields, ii) matches unconditional properties of the data, iii) is consistent with the level of news in expected inflation, and iv) passes the two requirements for a correct specification of term premia. Most of these features are also matched by reduced-form DTSMs, but these models offer little insights into the economic mechanisms that determine bond yields and especially term premia. The model we propose provides such a structural explanation, and this section analyzes the key mechanisms in $\mathcal{M}^{M,CS}$ that drive term premia. Our discussion is structured around Table 5, which

[17] In line with this finding, the Online Appendix further shows that $\mathcal{M}^{M,CS}$ also matches the short-rate expectations $\mathbb{E}_t[r_{t+1}]$ and $\mathbb{E}_t[r_{t+4}]$ in the Survey of Professional Forecasts.

Figure 3: The Ten-year Term Premia

The top figure shows the ten-year term premium in annualized basis points from $\mathcal{M}^{M,CS}$ and the model by Adrian et al. (2013). The bottom figure shows how each of the structural shocks in $\mathcal{M}^{M,CS}$ contributes to the variation in the ten-year term premium. The percentage of the total variation in the term premium explained by each shock, denoted $\text{pct}(\Delta TP_t)$, is computed based on the absolute variation in the series. The gray shaded bars denote NBER recessions, and term premium is expressed in annualized basis points.

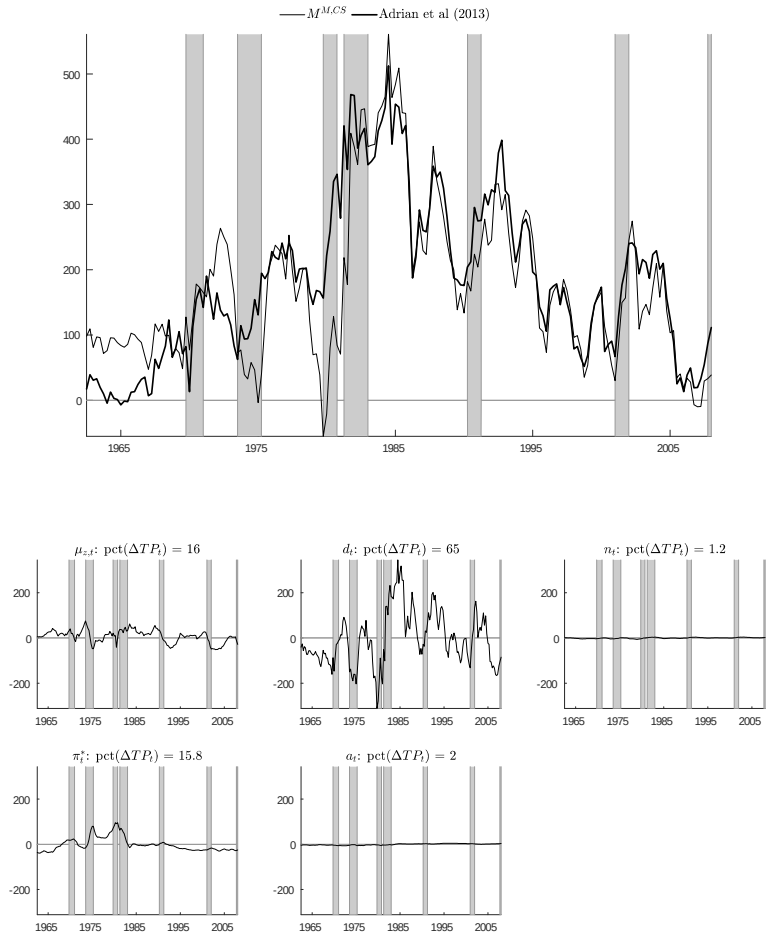

shows how unconditional moments and Campbell-Shiller loadings (both ordinary and risk-adjusted) are affected when omitting one of the five shocks in the model.

First, permanent productivity shocks have a large effect on bond yields. This is seen clearly from the unconditional means in Table 5, where omitting variation in $\mu_{z,t}$ (i.e. $\sigma_{\mu_z} = 0$) generates a strong steepening of the yield curve. For instance, the three-month bond yield falls from 5.68% to 2.61% and the ten-year bond yield increases from 6.97% to 10.53%. That

Table 5: Decomposing the Effects of the Structural Shocks

This table reports unconditional moments for $\mathcal{M}^{M,CS}$ when all structural shocks are present in column (1), and when each of the structural shocks are omitted in columns (2) to (6). The model-implied moments are computed in closed form based on Andreasen et al. (2018). All means and standard deviations are stated in annualized percent, except for the standard deviation of $\hat{l}_t$ which is not annualized.

	(1) $\mathcal{M}^{M,CS}$	(2) $\sigma_{\mu_z} = 0$	(3) $\sigma_d = 0$	(4) $\sigma_n = 0$	(5) $\sigma_{\pi^*} = 0$	(6) $\sigma_a = 0$
Means						
Δc_t	2.20	2.20	2.20	2.20	2.20	2.20
π_t	4.35	3.83	6.50	4.38	4.35	4.38
r_t	5.68	2.61	18.21	5.83	5.68	5.82
$r_t^{(4)}$	5.96	3.62	17.49	6.11	5.96	6.10
$r_t^{(12)}$	6.49	5.88	15.77	6.63	6.50	6.62
$r_t^{(20)}$	6.78	7.63	14.32	6.91	6.80	6.91
$r_t^{(28)}$	6.92	9.00	13.09	7.04	6.96	7.04
$r_t^{(40)}$	6.97	10.53	11.58	7.08	7.04	7.07
Stds						
$\hat{l}_t$	3.04	3.07	3.00	1.43	2.99	2.85
Δc_t	1.88	1.81	1.86	1.53	1.76	1.49
π_t	2.66	2.54	2.84	2.66	0.60	2.66
r_t	3.03	1.82	4.05	2.99	2.17	2.99
$r_t^{(4)}$	3.02	1.90	3.90	2.99	2.16	2.99
$r_t^{(12)}$	3.04	2.13	3.57	3.01	2.20	3.00
$r_t^{(20)}$	3.02	2.28	3.29	3.00	2.22	2.99
$r_t^{(28)}$	2.97	2.34	3.05	2.94	2.20	2.94
$r_t^{(40)}$	2.82	2.32	2.76	2.79	2.09	2.79
Ordinary CS loadings						
β_{12}	-1.04	-1.31	0.83	-1.04	-1.07	-1.04
β_{20}	-1.06	-1.48	0.85	-1.07	-1.11	-1.07
β_{28}	-1.04	-1.67	0.86	-1.04	-1.12	-1.04
β_{40}	-0.89	-1.99	0.88	-0.90	-1.05	-0.90
Adjusted CS loadings						
β_{12}^{Adj}	0.71	0.89	-1.34	0.97	0.56	0.78
β_{20}^{Adj}	0.77	1.05	-1.85	1.07	0.70	0.82
β_{28}^{Adj}	0.76	1.11	-2.32	1.08	0.79	0.80
β_{40}^{Adj}	0.62	1.05	-2.97	0.92	0.79	0.65

is, a permanent productivity shock generates a negative term premium. To understand why, observe from Figure 4 that a positive shock to $\mu_{z,t}$ increases consumption and raises inflation.[18] We therefore see a fall in the

[18] This increase in inflation is due to the high persistence of the shock and the induced

nominal stochastic discount factor $M_{t,t+1}$ that coincides with an increase in the long-term bond yield $r_t^{(40)}$, and hence a fall in the bond price $B_t^{(40)}$. As shown in Rudebusch and Swanson (2012), a positive comovement between $M_{t,t+1}$ and $B_t^{(40)}$ over the lifetime of the bond generates a negative term premium, and this explains why permanent productivity shocks help to flatten the yield curve. Table 5 also shows that permanent productivity shocks account for much of the variation in bond yields. For instance, the standard deviation in r_t falls from 3.03% to 1.82% and from 2.82% to 2.32% in $r_t^{(40)}$ when letting $\sigma_{\mu_z} = 0$. We also find that ordinary Campbell-Shiller loadings decrease without permanent technology shocks, for instance from -0.89 to -1.99 for $r_t^{(40)}$. This shows that permanent productivity shocks do not help to generate bond return predictability. The risk-adjusted Campbell-Shiller loadings are less affected by letting $\sigma_{\mu_z} = 0$ and remain close to one when omitting permanent productivity shocks.

Figure 4: A Permanent Productivity Shock

This figure shows the effects of a positive one-standard deviation shock to $\mu_{z,t}$ computed at the ergodic mean of the states using the results in Andreasen et al. (2018). Except for the nominal stochastic discount factor $M_{t,t+1}$, all impulse response functions are expressed in percentage deviations from the steady state (i.e. scaled by 100), with consumption expressed in deviations from the balanced growth path and all bond yields and inflation measured in annualized terms.

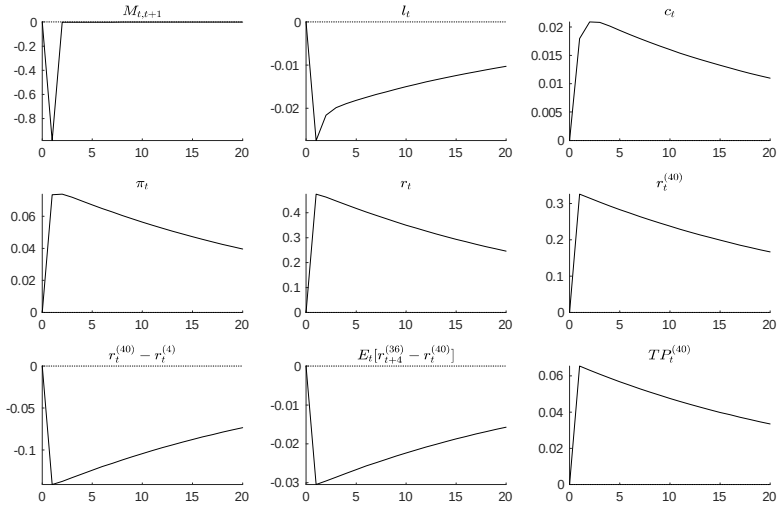

Second, demand shocks generate an upward sloping yield curve in $\mathcal{M}^{M,CS}$, as the third column in Table 5 shows that we get a strongly inverted yield

strong wealth effect. Hence, when $\rho_{\mu_z} = 0$, a positive shock to $\mu_{z,t}$ reduces inflation.

curve without these shocks (i.e. $\sigma_d = 0$). In contrast, demand shocks often generate a downward sloping yield curve in other versions of the New Keynesian model (see, for instance, Nakata and Tanaka (2016)). To understand this implication of $\mathcal{M}^{M,CS}$, consider the impulse response functions (IRFs) in Figure 5 for a positive demand shock in period $t+1$ computed at the ergodic mean of the states (the unmarked lines). We find that the demand shock increases consumption and inflation, but it also raises the long-term bond yield $r_t^{(40)}$, which is equivalent to a fall in $B_t^{(40)}$. Despite these responses, we see a large temporary *increase* in the nominal stochastic discount factor in the first period, because $d_{t+1}/d_t > 1$ and, more importantly, because d_{t+1} also scales the constant u_0 in the utility function. The latter generates a large increase in the value function V_{t+1}, which translates into a positive spike in $M_{t,t+1}$ through the term $\left(\mathbb{E}_t\left[V_{t+1}^{1-\alpha}\right]\right)^{\frac{\alpha}{1-\alpha}}/V_{t+1}^{\alpha}$ in (4). From the second period and onwards, this "surprise effect" in $M_{t,t+1}$ is no longer present, and $M_{t,t+1}$ therefore falls slightly below its steady state level. However, the large positive spike in $M_{t,t+1}$ in period one dominates the covariance between $M_{t,t+1}$ and the bond price $B_t^{(40)}$ over the lifetime of the bond, implying that demand shocks carry a positive term premium in $\mathcal{M}^{M,CS}$. This ability of demand shocks to generate an upward sloping yield curve is unrelated to conditional heteroskedasticity in these shocks, as we find the same comovement between $M_{t,t+1}$ and $r_t^{(40)}$ when $\omega_d = 0$, as shown by the dotted lines in Figure 5.[19]

Third, demand shocks are crucial for generating large and negative ordinary Campbell-Shiller loadings, as we find a large increase in these loadings when imposing $\sigma_d = 0$. For instance, β_{40} increases from -0.89 to 0.88 when omitting demand shocks. The risk-adjusted Campbell-Shiller loadings are also strongly affected and far from one, suggesting that term premia in $\mathcal{M}^{M,CS}$ no longer can explain deviations from the expectations hypothesis. We do not observe a similar large change in either the ordinary or the risk-adjusted Campbell-Shiller loadings when abstracting from any of the other shocks, implying that demand shocks are the main driver behind return predictability in $\mathcal{M}^{M,CS}$. To understand why demand shocks are crucial for matching the Campbell-Shiller loadings, consider once again the impulse response functions after a positive shock to d_t in Figure 5 at the ergodic mean of the states. We find higher consumption but only a small

[19] The Online Appendix shows that the same mechanism is present even when $u_0 = 0$, because d_t affects the utility of consumption *and* leisure in (2).

Figure 5: A Demand Shock

This figure shows the effects of a positive one-standard deviation shock to d_t computed using the results in Andreasen et al. (2018). Unless stated otherwise, the impulse responses are computed at the ergodic mean of the states. Except for the nominal stochastic discount factor $M_{t,t+1}$, all impulse response functions are expressed in percentage deviations from the steady state (i.e. scaled by 100), with consumption expressed in deviations from the balanced growth path and all bond yields and inflation measured in annualized terms.

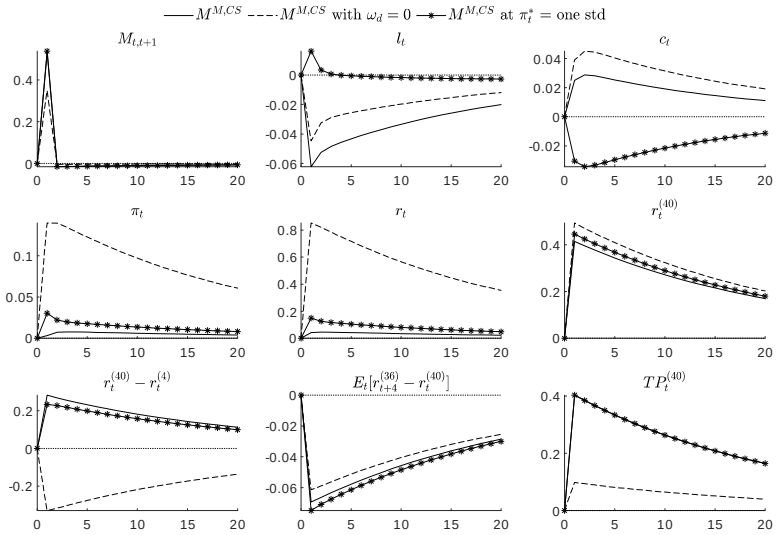

increase in inflation, which through the Taylor-rule generates a small positive response in the policy rate r_t. The average effect on inflation relative to the absolute change in consumption following the first eight periods after the shock (i.e. $\sum_{j=1}^{k} IRF_\pi(j) / \sum_{j=1}^{k} |IRF_c(j)|$) is only 0.27 in $\mathcal{M}^{M,CS}$, whereas it is 0.84 in the corresponding log-linearized version of the model estimated without the yield curve. This shows that bond yields are consistent with demand shocks that are three times less inflationary when using information from the yield curve. Figure 5 also plots the ten-year bond yield, which displays a much larger increase than the policy rate due to a rise in the term premium $TP_t^{(40)}$, and we therefore see an increase in the yield spread $r_t^{(40)} - r_t^{(4)}$. This coincides with a fall in the expected change in the ten-year yield $\mathbb{E}_t\left[r_{t+4}^{(36)}\right] - r_t^{(40)}$, implying that demand shocks generate a negative comovement between $\mathbb{E}_t\left[r_{t+4}^{(36)}\right] - r_t^{(40)}$ and $r_t^{(40)} - r_t^{(4)}$ as required to get a negative Campbell-Shiller loading.

To understand the contribution from conditional heteroskedasticity in demand shocks, consider the difference between the unmarked lines (i.e.

the full model) and the dotted lines with $\omega_d = 0$ in Figure 5. We see that higher uncertainty reduces the labor supply, consumption, inflation, and bond yields. These well-known negative effects of higher uncertainty are due to precautionary behavior, which encourage the household to consume less and work more if possible. With sticky prices, the lower consumption demand reduces output, which leads firms to demand less labor with higher uncertainty. In equilibrium, the price markup increases and the wage level falls (not shown), where the latter reduces marginal costs and hence inflation, as explained by Basu and Bundick (2017). Importantly, when uncertainty does not increase following a demand shock (i.e. $\omega_d = 0$), inflation and the policy rate r_t increase strongly, and we see a smaller increase in $r_t^{(40)}$ due to a more muted response in term premia. As a result, the yield spread $r_t^{(40)} - r_t^{(4)}$ falls after a demand shock, and we therefore get an undesirable positive comovement between $\mathbb{E}_t\left[r_{t+4}^{(36)}\right] - r_t^{(40)}$ and the yield spread when $\omega_d = 0$. This shows that demand shocks only help to generate negative Campbell-Shiller loadings because we allow for conditional heteroskedasticity in these shocks.

We have so far only discussed IRFs at the ergodic mean, but these responses generally depend on the state of the economy. This is illustrated in Figure 5, where we also show IRFs when the inflation target π_t^* is one standard deviation above its steady state level (the lines marked by stars), while the remaining states are at the ergodic mean. In such a high inflation environment where $\pi_t > \pi_{ss}$, an increase in inflation raises the output loss due to price stickiness $\frac{\xi}{2}\left(\frac{\pi_t}{\pi_{ss}} - 1\right)^2 y_t$. A positive demand shock therefore leads to a *fall* in consumption and a higher labor supply, whereas the responses in inflation and all bond yields are very similar to those discussed previously. Thus, in a high inflation environment, a demand shock generates a negative comovement between consumption and term premia, implying that demand shocks help to capture the stylized notion of countercyclical bond risk premia. By contrast, in a low inflation environment with $\pi_t < \pi_{ss}$ as seen around the ergodic mean, higher inflation reduces the output loss due to price stickiness $\frac{\xi}{2}\left(\frac{\pi_t}{\pi_{ss}} - 1\right)^2 y_t$, and this explains why a demand shock increases consumption and reduces labor supply in this case. Importantly, these radically different responses in consumption and labor supply are only present in a nonlinear model solution, and therefore not captured by the widely used log-linear approximation.

Finally, the last columns in Table 5 show that i) labor supply shocks n_t

explain much of the variation in the labor supply, ii) shocks to π_t^* control much of the variation in inflation and bond yields, and that iii) stationary productivity shocks a_t help to explain the variation in consumption growth.

5 Robustness Analysis

The results presented so far are obtained when shrinking the traditional QML estimates of the structural parameters towards some stylized empirical moments for $\mathbf{y}_t^{obs}$. Given that this estimator is new to the literature, Section 5.1 explores the effects of gradually eliminating this form of shrinkage. In the Online Appendix, we further show that the results in Section 4 are robust to i) omitting $r_t^{(4)}$, $r_t^{(12)}$, and $r_t^{(28)}$ from the estimation, ii) doubling the standard deviations for the measurement errors, iii) decreasing α in the utility function to -60, iv) increasing shrinkage to $\lambda = T \times 10$, and v) expanding the sample to include the zero lower bound period, which only has a small effect on the structural parameters as in Atkinson et al. (Forthcoming). The Online Appendix also shows, that our results are *not* robust to omitting heteroskedasticity in demand shocks with $\omega_d = 0$, as the model then becomes unable to jointly generate plausible inflation variance ratios and pass the two requirements for a correct specification of term premia.

5.1 The Effects of Shrinkage

To assess the impact of shrinkage, we first re-estimate the model when only shrinking the QML estimates to the first and second unconditional moments of $\mathbf{y}_t^{obs}$ and not to the ordinary Campbell-Shiller loadings. This version of the model is denoted $\mathcal{M}^M$. We find that this modification has a small effect on the structural parameters in Table 1, the model fit in Table 2, and the unconditional means and standard deviations in Table 3. The standard deviations of news to inflation and bond yields increase slightly, but the implied inflation variance ratios remain consistent with the data, as shown in Table 4. We further find that $\mathcal{M}^M$ generates bond return predictability with ordinary Campbell-Shiller loadings between -0.8 and -0.4, although these loadings are somewhat lower (in absolute terms) than in $\mathcal{M}^{M,CS}$ and the data. The risk-adjusted Campbell-Shiller loadings for $\mathcal{M}^M$ fall slightly compared to $\mathcal{M}^{M,CS}$, but their 95% confidence bands still

include the desired value of one.

Another possibility is to abstract from any shrinkage and simply use QML for the estimation. We refer to this version of the model as $\mathcal{M}$. This modification gives somewhat larger changes in the structural parameters - especially in b, χ, ξ_{Calvo}, ϕ_π, and ω_d (see Table 1). Also the changes in the labor supply shocks n_t and the inflation target shocks π_t^* are noteworthy, as they become more persistent and have higher conditional standard deviations. Table 2 shows that these estimates unexpectedly give a higher value of the quasi log-likelihood function when compared to $\mathcal{M}^{M,CS}$ and $\mathcal{M}^{M}$. However, this does not necessarily translate into smaller measurement errors, because $\mathcal{M}$ struggles to fit the evolution in inflation and short-term bond yields during the late 1970s and early 1980s. An even more disturbing shortcoming of not applying shrinkage is shown in Table 3, as $\mathcal{M}$ generates too much volatility in the observables $\mathbf{y}_t^{obs}$ with all standard deviations exceeding their 95% confidence bands. This implies that the standard deviations of news in expected inflation and bond yields are much larger than in the data according to Table 4. Thus, the standard QML estimates display signs of overfitting, as the improved value of the quasi log-likelihood function compared to $\mathcal{M}^{M,CS}$ and $\mathcal{M}^{M}$ comes at the cost of distorting the fit to several unconditional properties of the model. This also distorts estimates of term premia in $\mathcal{M}$, as its ordinary Campbell-Shiller loadings are close to one as implied by the expectation hypothesis.

6 Additional Model Implications

This section studies three additional implications of $\mathcal{M}^{M,CS}$ that are not included in the estimation, and hence can be considered as representing over-identified restrictions. First, demand shocks are a key driver behind bond risk premia in the model, but these shocks have also a direct effect on uncertainty when $\omega_d > 0$. Thus, one way to explore the plausibility of the proposed uncertainty channel is to study the conditional volatility in bond yields. This is done in Section 6.1. Second, the influential paper by Joslin et al. (2014) criticizes a wide class of macro-finance term structure models because they are unable to address the so-called "spanning puzzle". We summarize the arguments of Joslin et al. (2014) in Section 6.2 and explore whether $\mathcal{M}^{M,CS}$ can explain this puzzle. Third, the ability of the model to match key moments for equity returns are finally discussed in Section 6.3,

although the model has *not* been constructed for this purpose.[20]

6.1 Conditional Volatilities

Figure 6 plots the historical evolution in the quarterly volatilities and their 95% confidence bands at the tree-, five-, and ten-year maturity when estimated by the EGARCH(1,1) model of Nielson (1991) applied to the change in yields.[21] For the New Keynesian model, we simulate bond yields one quarter forward at each estimated state by the CDKF and report the standard deviations. Figure 6 shows that these model-implied volatilities generally tract the empirical volatilities fairly closely with correlations between 0.7 and 0.8. The main exception is in the early 1980s, where the New Keynesian model is unable to generate a sufficiently large increase in volatility.

Table 6 summarizes some stylized moments for the conditional volatility at the ten-year maturity, where the model-implied moment are obtained from a simulated sample of $10,000$ observations. Panel $\mathcal{A}$ shows that the empirical volatilities for the short rate $\hat{\sigma}_t^{(1)}$ and the ten-year yield $\hat{\sigma}_t^{(40)}$ display a strong positive correlation of 0.75. The same holds in our model where the corresponding correlation is 0.88. Panel $\mathcal{B}$ reveals that $\hat{\sigma}_t^{(40)}$ is strongly correlated with the level of ten-year bond yield (0.91), and that we find the same correlation in the New Keynesian model. We further see from Panel $\mathcal{C}$ that the yield spread does not predict the volatility in the ten-year yield $\hat{\sigma}_t^{(40)}$, both in the data and in the model. The ability of $\hat{\sigma}_t^{(40)}$ to forecast annual excess returns at the ten-year maturity $rx_t^{(40)}$ when controlling for the yield spread is considered in Panel $\mathcal{D}$. We find that $\hat{\sigma}_t^{(40)}$ has predictive power for $rx_t^{(40)}$ with a slope coefficient of 13.66, which is statistical significant at a 1% level with a t-statistic of 2.64. However, the presence of estimation noise in $\hat{\sigma}_t^{(40)}$ implies that the second moment of $\hat{\sigma}_t^{(40)}$ exceeds the second moment of the true (but infeasible) volatility $\sigma_t^{(40)}$, implying that this slope coefficient is biased towards zero. A simple way to correct for this bias is to generate $\mathcal{S}$ sample paths of U.S. volatility by using the as-

[20] The model $\mathcal{M}^{M,CS}$ generates also an upward sloping real yield curve and a positive inflation risk premium as typically found for the U.S. economy. These effects are due to demand shocks and arises for the same reason as described above for the nominal yield curve. We therefore delegate this analysis to the Online Appendix.

[21] Unreported results show that the EGARCH(1,1) model is better than the widely used GARCH(1,1) model to capture the conditional volatilities in bond yields, in part because the imposed parameter restrictions in the GARCH(1,1) model to ensure non-negative volatililty and stability are binding.

Figure 6: Historical Plots of Conditional Volatility in Bond Yields

This figure shows the implied one-step ahead conditional volatilities in bond yields. The volatilities in the data are measured by the EGARCH(1,1) model of Nelson (1991) applied to the change in bond yields. The shaded area denotes the 95 percent confidence interval for the volatility estimate in this model. For the New Keynesian model $\mathcal{M}^{M,CS}$, we condition on a given estimated state from the CDKF, simulate 2,000 realizations of bond yields, and report their standard deviations.

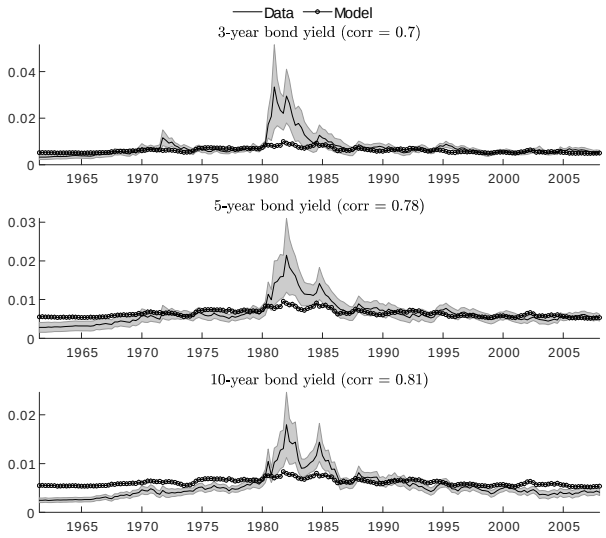

ymptotic distribution for the parameters in the EGARCH(1,1) model and estimate the bias by $\hat{B}_\sigma = \sum_{s=1}^{\mathcal{S}} \sum_{t=1}^{T} \left(\sigma_{t,s}^{(40)}\right)^2 / \mathcal{S} - \sum_{t=1}^{T} \left(\hat{\sigma}_t^{(40)}\right)^2$. The bias-adjusted OLS estimator is then given by $(\mathbf{X}'\mathbf{X} - \mathbf{B})^{-1}\mathbf{X}'\mathbf{Y}$, where $\mathbf{X} \equiv \left[\begin{array}{ccc} \mathbf{1}_T & \mathbf{r}_{1:T}^{(40)} - \mathbf{r}_{1:T}^{(4)} & \hat{\boldsymbol{\sigma}}_{1:T}^{(40)} \end{array} \right]$ is the $T \times 3$ data matrix for the regressors, $\mathbf{Y}$ is the $T \times 1$ data matrix for the dependent variable, and $\mathbf{B} = \mathbf{0}$ except for $B(3,3) = \hat{B}_\sigma$.[22] The bottom part of Table 6 shows that this adjustment increases the slope coefficient for $\hat{\sigma}_t^{(40)}$ to 16.61 and raises its t-statistic to 3.27. The model-implied slope coefficient is 23.1 and hence well inside the 95% confidence interval $[6.7, 26, 5]$ for the bias-adjusted empirical slope coefficient. Note also that imposing $\omega_d = 0$ in the model implies a too low slope coefficient for $\sigma_t^{(40)}$ of 3.90, in addition to a negative effect of the yield spread on excess bond returns.

Another and more indirect way to evaluate the plausibility of the conditional volatility in bond yields is to compute quarterly Sharpe ratios.

[22] A similar correction is applied to the Newey-West standard errors reported in Table 6.

Table 6: Stylized Properties of Conditional Volatility

This table reports stylized moments for the one-step ahead conditional volatility in the ten-year bond yield, denoted $\hat{\sigma}_t^{(40)}$. The conditional volatility in the data is measured by the EGARCH(1,1) model of Nelson (1991) applied to the change in the ten-year bond yield. In the New Keynesian model, conditional volatility at a given state $\mathbf{x}_t$ is computed as the standard deviation of 2,000 bond yields simulated one period forward. The reported moments for the New Keynesian model are computed using a simulated sample of 10,000 observations for the conditional volatility and bond yields. The reported moments are for the slope coefficient. In Panel $\mathcal{A}$ and $\mathcal{B}$, the regressand and the regressors are normalized to have a zero mean and a unit variance. Figures in parenthesis for the data moments refer to Newey-West standard errors computed using one lag in Panel $\mathcal{A}$ to Panel $\mathcal{C}$ and five lags in Panel $\mathcal{D}$. Significance at the 10 and 5 percent level are denoted by ** and *, respectively.

	Data	Model	
		$\mathcal{M}^{M,CS}$	$\mathcal{M}^{M,CS}$ with $\omega_d = 0$
Panel $\mathcal{A}$: Comovement between volatilities			
$\hat{\sigma}_t^{(40)} = \alpha + \beta\hat{\sigma}_t^{(1)} + u_t$	0.75^{**} (0.12)	0.88	0.93
Panel $\mathcal{B}$: Volatility and its level			
$\hat{\sigma}_t^{(40)} = \alpha + \beta r_t^{(40)} + u_t$	0.91^{**} (0.06)	0.91	0.85
Panel $\mathcal{C}$: Volatility predictability			
$\hat{\sigma}_{t+1}^{(40)} = \alpha + \beta\left(r_t^{(40)} - r_t^{(4)}\right) + u_{t+1}$	-0.02 (0.03)	0.02	-0.02
Panel $\mathcal{D}$: Bond return predictability			
$rx_{t+4}^{(40)} = \alpha + \beta\left(r_t^{(40)} - r_t^{(4)}\right) + \delta\hat{\sigma}_t^{(40)} + u_{t+4}$			
β	3.48^{**} (0.97)	1.57	-0.52
δ	13.66^{**} (5.18)	23.09	3.90
β with bias-adjustment	3.50^{**} (0.96)	-	-
δ with bias-adjustment	16.61^{**} (5.07)	-	-

For a k-period bond at time t, the conditional Sharpe ratio is defined as $SR_t^{(k)} \equiv \mathbb{E}_t\left[R_{t+1}^{(k)} - R_{t+1}^{(1)}\right] / \sqrt{\mathbb{V}_t\left[R_{t+1}^{(k)} - R_{t+1}^{(1)}\right]}$, where $R_{t+1}^{(k)} \equiv P_{t+1}^{(k-1)}/P_t^{(k)}$. To compute $SR_t^{(k)}$ in the New Keynesian model, we first simulate a sample of $10,000$ states, i.e. $\{\mathbf{x}_t\}_{t=1}^{10,000}$. At a given state $\mathbf{x}_t$, we then simulate $2,000$ realizations of bond yields and excess returns to compute $SR_t^{(k)}$. The mean of these conditional Sharpe ratios are 0.31, 0.21, 0.15, and 0.08 at the one-, three-, five-, and ten-year maturity. Their overall level are thus consistent with the empirical evidence in Pilotte and Sterbenz (2006), and so is the decreasing pattern in $SR_t^{(k)}$ with maturity.

Thus, the conditional volatility in bond yields are well matched by $\mathcal{M}^{M,CS}$, although none of these volatilities are included directly in the estimation.

6.2 The Yield Curve and Spanned Macro Variation

Many DTSMs with macro variables imply that bond yields are a linear combination of latent factors and observed macro variables. This linear mapping can (up to knife-edge restrictions) be inverted to express macro variables as a function of bond yields. All variation in macro variables is therefore spanned (i.e. explained) by bond yields. However, this implication is heavily criticized by Joslin et al. (2014) because regressions of macro variables on linear combination of bond yields (i.e. the principal components) typically generate R^2 values substantially below one. This constitutes the "spanning puzzle", which leads Joslin et al. (2014) to challenge the usefulness of most equilibrium models - including the standard New Keynesian model. The model we propose also implies that bond yields depend on macro variables, but this relation is not linear. Thus, the nonlinear structure of our model may generate what may appear to be unspanned variation in macro variables and hence resolve the spanning puzzle.

We explore this possibility in Table 7 by regressing each of the three macro variables included in the estimation of the model on the first K principal components of bond yields. The model $\mathcal{M}^{M,CS}$ has five structural shocks, suggesting that at least five principal components are required to span variation in the macro variables. The first column in Table 7 shows that U.S. bond yields only explain a fairly small proportion of the variation in the labor supply $\hat{l}_t$ (19.2%) and consumption growth Δc_t (22.2%), whereas inflation π_t displays some evidence of spanning with an R^2 of 60.3%. The results for the New Keynesian model are largely consistent with these regressions according to the second column in Table 7, where the corresponding values of the R^2 are 4.1% for $\hat{l}_t$, 8.4% for Δc_t, and 70.1% for π_t. These figures are computed using a simulated sample of $100,000$ observations that include the same measurement errors $\mathbf{v}_t$ as applied when estimating $\mathcal{M}^{M,CS}$. Measurement errors help to generate unspanned variation, as emphasized in Bauer and Rudebusch (2017), and we therefore omit these errors in the third column of Table 7. The R^2 values then increase slightly to 9.3% for $\hat{l}_t$ and 20.2% for Δc_t, while inflation now basically is

Table 7: Regression Evidence on the Spanning Hypothesis

This table shows the R^2 in percent from the regression $m_t = \alpha + \beta' \mathbf{pca}_t^{(K)} + u_t$, where m_t refers to a macro variable and $\mathbf{pca}_t^{(K)}$ of dimension $K \times 1$ contains the first K principal components of bond yields. The R^2s in the data are provided in column (1) and computed on U.S. data from 1961 Q2 to 2007 Q4, with the 95 percent confidence interval (shown below the estimate) computed using a block bootstrap, where the regressand and the regressors are sampled jointly in blocks of 50 observations in 10,000 bootstrap samples. The corresponding R^2s implied by the New Keynesian model $\mathcal{M}^{M,CS}$ are computed using a simulated sample of 100,000 observations. The simulated sample in column (2) is obtained using the nonlinear model solution (i.e. third order perturbation) and with measurement errors for macro variables and bond yields of the same size as considered in the estimation. The same nonlinear model solution is used in column (3), but no measurement errors are added to the macro variables and bond yields. The simulated sample in column (4) uses a simplified third-order perturbation approximation, where all terms that are quadratic and cubic in the states are omitted to get a risk-adjusted linear approximation without measurement errors.

	(1) Data	(2) Nonlinear model & Measurement errors	(3) Nonlinear model	(4) Linear model
$K = 5$				
$\hat{l}_t$	19.2 [9.2,68.9]	4.1	9.3	24.7
Δc_t	22.2 [7.2,44.2]	8.4	20.2	83.7
π_t	60.3 [41.1,82.9]	70.1	95.5	99.7
$K = 6$				
$\hat{l}_t$	19.5 [9.4,70.3]	4.1	13.7	100.0
Δc_t	22.4 [7.4,44.2]	8.4	21.2	100.0
π_t	60.5 [40.5,83.4]	70.1	96.2	100.0

spanned with an R^2 of 95.5%.

To evaluate the degree of unspanned variation that is generated by the nonlinear structure of the New Keynesian model, the fourth column in Table 7 reports the R^2 values when using a risk-adjusted linear solution to the model. This solution is computed by omitting terms in the approximation of the **g**- and **h**-functions that are quadratic and cubic in the states. The R^2 values now increase to 24.7% for $\hat{l}_t$, 83.7% for Δc_t, and 99.7% for π_t. We do not achieve perfect spanning (i.e. $R^2 = 1$) in this case because consumption habits and conditional heteroskedasticity in d_t introduce $\log c_{t-1}$ and $\log d_{t-1}$, respectively, as endogenous states. The last part of Table 7 shows that an additional principal component with $K = 6$ allows us to capture the information in these endogenous states and achieve perfect spanning.

Accordingly, the nonlinear structure of the New Keynesian model implies that bond yields only explain a fairly small proportion of the variation in $\hat{l}_t$ (13.7%) and Δc_t (21.2%), which is in line with U.S. data. For inflation, the nonlinearities in the model have a somewhat smaller effect, and measurement errors are therefore needed to achieve a sufficiently low R^2 of 70.1% that lies well within the 95% confidence interval for the explained variation in U.S. inflation. Thus, the proposed model is to a large extent able to resolve the spanning puzzle. This result may also serve as a more theoretical motivation for imposing the restrictions in Joslin et al. (2014), because these restrictions make their reduced-form DTSM more consistent with an equilibrium model of the type proposed in this paper.

6.3 Equity Returns

We define the market return r_t^m as a claim on firm dividends D_t. This implies that the real market price P_t^m is given by $1 = \mathbb{E}_t\left[M_{t,t+1}^{real} e^{r_{t+1}^m}\right]$, where $e^{r_{t+1}^m} = \left(D_{t+1} + P_{t+1}^m\right)/P_t^m$, $M_{t,t+1}^{real} = M_{t,t+1}\pi_{t+1}$, and $D_t = y_t - w_t l_t - \frac{1}{2}\xi\left(\pi_t/\pi_{ss} - 1\right)^2 y_t - z_t \delta k_{ss}$. To account for leverage as present in the data, excess market returns are modeled as $r_t^{ex} = \omega^{lev}\left(r_t^m - r_t^{real}\right)$ with $\omega^{lev} = 2$ as in Croce (2014). In $\mathcal{M}^{M,CS}$, r_t^{ex} has a mean of 6.2% and a standard deviation of 19.7%. This is very similar to the corresponding moments for the U.S. of about 6% and 20% (see, for instance, Beeler and Campbell (2012) and Croce (2014)).

Another set of stylized properties for equity returns relate to their predictability. Panel $\mathcal{A}$ in Table 8 shows that the ten-year yield spread $r_t^{(40)} - r_t^{(4)}$ in the U.S. predicts significant higher excess equity returns two and three years in the future. The second column in Table 8 shows that this predictability result is captured by $\mathcal{M}^{M,CS}$, which generates regression coefficients and values of the R^2 that match those obtained in the data. The presence of conditional heteroskedasticity in demand shocks is here essential, as imposing $\omega_d = 0$ in $\mathcal{M}^{M,CS}$ generates forecasts with the wrong sign. The last column in Table 8 further shows that it is demand shocks that enable the yield spread to predict equity returns in $\mathcal{M}^{M,CS}$, as omitting these shocks ($\sigma_d = 0$) generate R^2 values in these predictability regressions that are basically zero.

Following the work of Fama and French (1989), Panel $\mathcal{B}$ in Table 8 uses both the yield spread and the log-transformed price-dividend ratio pd_t

Table 8: Return Predictability in Equity Returns

Panel $\mathcal{A}$ shows the regression coefficients and the R^2 in percent when regressing future excess equity returns on the slope of the yield curve. Panel $\mathcal{B}$ extends this regression with the price-dividend ratio (pd_t). For the empirical data moments, these regressions are computed on U.S. data from 1961 Q2 to 2007 Q4, where the price-dividend ratio and the excess equity return are computed as in Beeler and Campbell (2012). Figures in parenthesis for the data moments refer to Newey-West standard errors computed using $j+1$ lags. Significance at the 10 and 5 percent level are denoted by ** and *, respectively. The corresponding moments in the model are computed on a simulated sample of 100,000 observations using the estimates for $\mathcal{M}^{M,CS}$, except when stated otherwise. All variables in the two regressions are demeaned and scaled to have a unit standard deviation.

		Model: $\mathcal{M}^{M,CS}$		
	(1) Data	(2) Full version	(3) $\omega_d = 0$	(4) $\sigma_d = 0$
Panel $\mathcal{A}$:				
$\sum_{i=1}^{j} r_{t+i}^{ex} = \alpha_j + \beta_j \left(r_t^{(40)} - r_t^{(4)} \right) + \upsilon_{t+j}$				
β_4	0.31 (0.23)	0.33	-0.15	0.04
β_8	0.52** (0.20)	0.61	-0.27	0.08
β_{12}	0.75** (0.23)	0.84	-0.38	0.13
R_4^2	2.6	3.0	0.6	0.0
R_8^2	4.0	5.2	1.0	0.1
R_{12}^2	6.4	7.0	1.3	0.1
Panel $\mathcal{B}$:				
$\sum_{i=1}^{j} r_{t+i}^{ex} = \alpha_j + \beta_j \left(r_t^{(40)} - r_t^{(4)} \right) + \delta_j pd_t + \upsilon_{t+j}$				
β_4	0.42* (0.23)	0.18	-0.12	0.15
β_8	0.72** (0.29)	0.33	-0.23	0.30
β_{12}	1.01** (0.29)	0.46	-0.34	0.44
δ_4	−0.42 (0.27)	-0.39	-0.03	-0.19
δ_8	−0.71 (0.48)	-0.73	-0.04	-0.37
δ_{12}	−0.90* (0.50)	-1.01	-0.05	-0.53
R_4^2	6.8	6.5	0.6	0.6
R_8^2	10.7	11.5	1.0	1.2
R_{12}^2	14.3	15.6	1.3	1.6

to forecast future equity returns. A higher price-dividend ratio forecasts negative future equity returns, as typically found in the literature, although this effect is not strongly significant in our sample. The model matches this predictability result with regression loadings for pd_t that closely match

those in our sample and hence basically produces the same R^2 values as in the data. Again, demand shocks with heteroskedasticity are key for obtaining these results, as seen from the two last columns in Table 8.

Thus, the proposed New Keynesian model matches several stylized properties of equity returns, although these moments are not included in the estimation. We showed in Section 4.7 that demand shocks d_t enable the yield spread to match ordinary Campbell-Shiller loadings and predict excess bond returns, and this section shows that these shocks also allow the yield spread to predict excess equity returns. Our model therefore rationalizes the old conjecture in Fama and French (1989) that the yield spread forecasts future bond and equity returns due to shocks to the discount rate, as captured by variation in d_t within our model.

7 Conclusion

This paper addresses a long-standing ambition in the literature by formulating a New Keynesian model to provide a structural explanation for variation in bond yields and their risk premia. The key innovation is to introduce demand shocks, where the conditional variance increases with the level of these shocks. This uncertainty channel reduces the inflationary effect of a demand shock and generates bond yields with a low level of news in expected inflation. These demand shocks also enable the model to pass two requirements for a correct specification of term premia and explain several unconditional properties of bond yields. It is obvious that we have only scratched the surface when it comes to analyzing the macroeconomic implications of no longer ignoring financial assets. For instance, studying optimal monetary and fiscal policy responses in a setting with properly specified risk corrections seem particularly promissing, as these policies depend strongly on higher-order terms in the model solution. We leave these and other applications for future work.

References

Adrian, T., Crump, R. K. and Moench, E. (2013), 'Pricing the Term Structure with Linear Regressions', *Journal of Financial Economics* **110**(1), 110–138.

Albuquerque, R., Eichenbaum, M., Luo, V. X. and Rebelo, S. (2016), 'Valuation Risk and Asset Pricing', *Journal of Finance* **71**(6), 2861–2904.

Andreasen, M. M. (2013), 'Non-Linear DSGE Models and the Central Difference Kalman Filter', *Journal of Applied Econometrics* **28**, 929–955.

Andreasen, M. M., Fernandez-Villaverde, J. and Rubio-Ramirez, J. F. (2018), 'The Pruned State Space System for Non-Linear DSGE Models: Theory and Empirical Applications to Estimation', *Review of Economic Studies* **85**(1), 1–49.

Andreasen, M. M. and Jørgensen, K. (2020), 'The Importance of Timing Attitudes in Consumption-Based Asset Pricing Models', *Journal of Monetary Economics* **111**, 95–117.

Atkinson, T., Richter, A. W. and Throckmorton, N. A. (Forthcoming), 'The Zero Lower Bound and Estimation Accuracy', *Journal of Monetary Economics* .

Bansal, R. and Yaron, A. (2004), 'Risks for the Long Run: A Potential Resolution of Asset Pricing Puzzles', *Journal of Finance* **59**(4), 1481–1509.

Basu, S. and Bundick, B. (2017), 'Uncertainty Shocks in a Model of Effective Demand', *Econometrica* **85**(3), 937–958.

Bauer, M. D. and Rudebusch, G. D. (2017), 'Resolving the Spanning Puzzle in Macro-Finance Term Structure Models', *Review of Finance* **21**(2), 511–553.

Beeler, J. and Campbell, J. Y. (2012), 'The Long-Run Risks Model and Aggregate Asset Prices: An Empirical Assessment', *Critical Finance Review* **1**(1), 141–182.

Benigno, P. (2007), *Discussion of "Equilibrium Yield Curves" by Monika Piazzesi and Martin Schneider, in: NBER Macroeconomics annual*, Vol. 21, Cambridge MA: MIT press.

Campbell, J. Y. and Shiller, R. J. (1991), 'Yield Spread and Interest Rate Movements: A Bird's Eye View', *The Review of Economic Studies* **58**(3), 495–514.

Chernozhukov, V. and Hong, H. (2003), 'An MCMC Approach to Classical Estimation', *Journal of Econometrics* **115**(2), 293–346.

Christiano, L. J., Trabandt, M. and Walentin, K. (2011), 'Introducing Financial Frictions and Unemployment into a Small Open Economy Model', *Journal of Economic Dynamic and Control* **35**(12), 1999–2041.

Cochrane, J. H. (2007), 'Financial Markets and the Real Economy', *Handbook of the equity risk premium, Chapter 7* pp. 237–330.

Croce, M. M. (2014), 'Long-Run Productivity Risk: A New Hope for Production-Based Asset Pricing?', *Journal of Monetary Economics* **66**, 13–31.

Dai, Q. and Singleton, K. J. (2002), 'Expectation Puzzles, Time-Varying Risk Premia and Affine Models of the Term Structure', *Journal of Financial Economics* **63**(3), 415–441.

Duffee, G. R. (2018), 'Expected Inflation and Other Determinants of Treasury Yields', *The Journal of Finance* **73**(5), 2139–2180.

Epstein, L. G., Farhi, E. and Strzalecki, T. (2014), 'How Much Would You Pay to Resolve Long-Run Risk?', *American Economic Review* **104**(9), 2680–2697.

Epstein, L. G. and Zin, S. E. (1989), 'Substitution, Risk Aversion, and the Temporal Behavior of Consumption and Asset Returns: A Theoretical Framework', *Econometrica* **57**(4), 937–969.

Fama, E. F. and French, K. R. (1989), 'Business Conditions and Expected Returns on Stocks and Bonds', *Journal of Financial Economics* **25**(1), 23–49.

Fernández-Villaverde, J. and Rubio-Ramírez, J. F. (2007), 'Estimating Macroeconomic Models: A Likelihood Approach', *Review of Economic Studies* **74**(4), 1–46.

Gomez-Cram, R. and Yaron, A. (forthcoming), 'How Important are Inflation Expectations for the Nominal Yield Curve?', *The Review of Financial Studies* .

Gürkaynak, R., Sack, B. and Wright, J. (2007), 'The U.S. Treasury Yield Curve: 1961 to the Present', *Journal of Monetary Economics* **54**(8), 2291–2304.

Hall, R. E. (1988), 'Intertemporal Substitution in Consumption', *Journal of Political Economy* **96**(2), 339–357.

Hamilton, J. D. (2018), 'Why You Should Never Use the Hodrick-Prescott Filter', *The Review of Economics and Statistics* **100**(5), 831–843.

Hansen, L. P. (1982), 'Large Sample Properties of Generalized Method of Moments Estimators', *Econometrica* **50**(4), 1029–1054.

Joslin, S., Priebsch, M. A. and Singleton, K. J. (2014), 'Risk Premiums in Dynamic Term Structure Models with Unspanned Macro Risks', *The Journal of Finance* **69**(3), 1197–1233.

Keane, M. P. (2011), 'Labor Supply and Taxes: A Survey', *Journal of Economic Literature* **49**(4), 961–1075.

Kreps, D. M. and Porteus, E. L. (1978), 'Temporal Resolution of Uncertainty and Dynamic Choice Theory', *Econometrica* **46**(1), 185–200.

Kung, H. (2015), 'Macroeconomic Linkages between Monetary Policy and the Term Structure of Interest Rates', *Journal of Financial Economics* **115**(1), 42–57.

Nakata, T. and Tanaka, H. (2016), 'Equilibrium Yield Curves and the Interest Rate Lower Bound', *Finance and Economic Discussion Series, Federal Reserve Board, Washington D. C.* .

Nielson, D. B. (1991), 'Conditional heteroskedasticity in asset returns: A new approach', *Econometrica* **59 No. 2**, 347–370.

Norgaard, M., Poulsen, N. K. and Ravn, O. (2000), 'Advances in Derivative-Free State Estimation for Nonlinear Systems', *Automatica* **36**(11), 1627–1638.

Piazzesi, M. and Schneider, M. (2007), *Equilibrium Yield Curves, in NBER Macroeconomics Annual 2006*, Vol. 21, Cambridge MA: MIT press.

Pilotte, E. A. and Sterbenz, F. P. (2006), 'Sharpe and Treynor Ratios on Treasury Bonds', *The Journal of Business* **79**(1), 149–180.

Rotemberg, J. J. (1982), 'Monopolistic Price Adjustment and Aggregate Output', *Review of Economic Studies* **49**, 517–531.

Rudebusch, G. D. (2002), 'Term Structure Evidence on Interest Rate Smoothing and Monetary Policy Inertia', *Journal of Monetary Economics* **49**(6), 1161–1187.

Rudebusch, G. D. and Swanson, E. T. (2012), 'The Bond Premium in a DSGE Model with Long-Run Real and Nominal Risks', *American Economic Journal: Macroeconomics* **4**(1), 1–43.

Swanson, E. T. (2018), 'Risk Aversion, Risk Premia, and the Labor Margin with Generalized Recursive Preferences', *Review of Economic Dynamics* **28**, 290–321.

Weil, P. (1990), 'Nonexpected Utility in Macroeconomics', *Quarterly Journal of Economics* **105**(1), 29–42.

Yogo, M. (2004), 'Estimating the Elasticity of Intertemporal Substitution When Instruments Are Weak', *The Review of Economics and Statistics* **86**(3), 797–810.

Research Papers 2021

CREATES
Center for Research in Econometric Analysis of Time Series

2020-05: Juan Carlos Parra-Alvarez, Olaf Posch and Mu-Chun Wang: Estimation of heterogeneous agent models: A likelihood approach

2020-06: James G. MacKinnon, Morten Ørregaard Nielsen and Matthew D. Webb: Wild Bootstrap and Asymptotic Inference with Multiway Clustering

2020-07: Javier Hualde and Morten Ørregaard Nielsen: Truncated sum of squares estimation of fractional time series models with deterministic trends

2020-08: Giuseppe Cavaliere, Morten Ørregaard Nielsen and Robert Taylor: Adaptive Inference in Heteroskedastic Fractional Time Series Models

2020-09: Daniel Borup, Jonas N. Eriksen, Mads M. Kjær and Martin Thyrsgaard: Predicting bond return predictability

2020-10: Alfonso A. Irarrazabal, Lin Ma and Juan Carlos Parra-Alvarez: Optimal Asset Allocation for Commodity Sovereign Wealth Funds

2020-11: Bent Jesper Christensen, Juan Carlos Parra-Alvarez and Rafael Serrano: Optimal control of investment, premium and deductible for a non-life insurance company

2020-12: Anine E. Bolko, Kim Christensen, Mikko S. Pakkanen and Bezirgen Veliyev: Roughness in spot variance? A GMM approach for estimation of fractional log-normal stochastic volatility models using realized measures

2020-13: Morten Ørregaard Nielsen and Antoine L. Noël: To infinity and beyond: Efficient computation of ARCH(∞) models

2020-14: Charlotte Christiansen, Ran Xing and Yue Xu: Origins of Mutual Fund Skill: Market versus Accounting Based Asset Pricing Anomalies

2020-15: Carlos Vladimir Rodríguez-Caballero and J. Eduardo Vera-Valdés: Air pollution and mobility in the Mexico City Metropolitan Area, what drives the COVID-19 death toll?

2020-16: J. Eduardo Vera-Valdés: Temperature Anomalies, Long Memory, and Aggregation

2020-17: Jesús-Adrián Álvarez, Malene Kallestrup-Lamb and Søren Kjærgaard: Linking retirement age to life expectancy does not lessen the demographic implications of unequal lifespans

2020-18: Mikkel Bennedsen, Eric Hillebrand and Siem Jan Koopman: A statistical model of the global carbon budget

2020-19: Eric Hillebrand, Jakob Mikkelsen, Lars Spreng and Giovanni Urga: Exchange Rates and Macroeconomic Fundamentals: Evidence of Instabilities from Time-Varying Factor Loadings

2021-01: Martin M. Andreasen: The New Keynesian Model and Bond Yields